Cruise report, expedition 64PE525
Texel – Texel, the Netherlands (15-10 – 01-11-2023)

Helge Niemann[1,2], Annalisa Delre[1], Yasmina Ourradi[1], Ilona Velzeboer[3], Henk de Haas[1], Noortje Versteijlen[3], Pepien Rubbens[1,2], Jessica Riekenberg[1], Robin Lindy van Dijk[4], Jesper Volmer[5]

[1]Royal Netherlands Institute for Sea Research (NIOZ)
[2]Utrecht University
[3]TNO
[4]University Groningen
[5]SodM

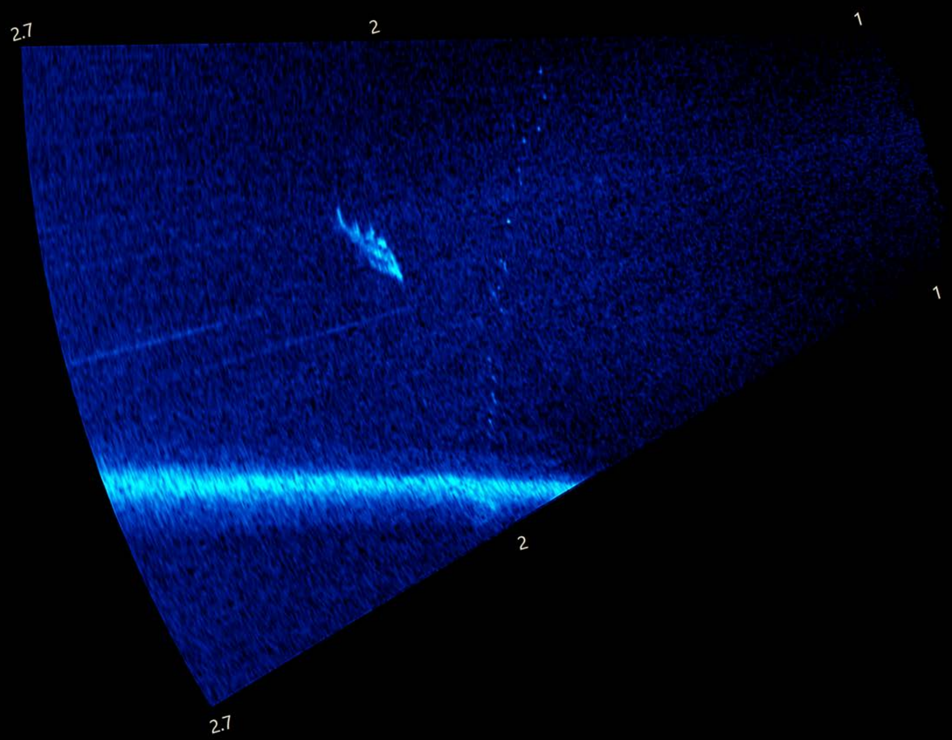

Contents

General introduction and expedition goals

Helge Niemann, Chief Scientist

Methane (CH_4) is an important greenhouse gas, that is 32 times more potent than CO_2 on a time horizon of 100 years (Etminan et al., 2016). Though the half-life of atmospheric methane is relatively short (~ 9 years), CH_4 concentrations in the atmosphere have risen drastically to current values of ~ 1.9 ppm; i.e. ~ 2.5-fold higher compared to preindustrial values (IPCC, 2021). The exact mechanisms behind this increase are not fully understood, yet it is clear that the increase in the atmospheric methane budget is caused by anthropogenic sources (Nisbet et al., 2019); together, these amount to 336 - 376 Tg yr^{-1}. Natural CH_4 sources are overall on a similar scale contributing about 40% (183–248 Tg yr^{-1}) to the total atmospheric budget (Saunois et al., 2020; IPCC, 2021).

Though it is likely that the overall contribution of the Ocean to the atmospheric methane content is comparably small, ocean budget estimates vary considerably. Shelf seas for example are with 9 - 22 Tg yr^{-1} the main contributor of natural oceanic methane emission to the atmosphere though the shelf only accounts for 8 - 10 % of the global ocean surface (Weber et al., 2019; Saunois et al., 2020). Compared to the open ocean, shelf seas are characterized by high nutrient loads, high primary production, high sedimentation rates and subsequent burial of dead organic matter to the seabed. This leads to elevated methane production in sediments by microbial or thermogenic processes (Reeburgh, 2007). Methane emission related to offshore industries on the other hand are virtually unknown. However, methane in shelf sea sediments is of commercial value and thus extracted. After exploitation, wells are sealed to prevent leakage, but recent investigations in the UK and German sector of the North Sea by Vielstädte et al. (2017) and Böttner et al. (2020), however, found acoustic flares in the water column in vicinity of well heads; these acoustic features are caused by plumes of rising bubbles emanating from the sea floor. The authors almost always found such flares if the well heads were above bright spots in seismic data. Bright spots are caused by high amplitude response in sound velocity of the subsurface, e.g. triggered by the presence of shallow gas. These previous studies could not fully clarify why the location of sea floor gas release was often at some distance from the well head (i.e. the leak-tightness of the well head seal itself was not necessarily compromised). However, the statistical co-occurrence of flares and (abandoned) wells suggested a causality.

The Dutch sector of the North Sea is rich in shallow and deep subsurface methane. The deep methane is extracted from multiple active wells and many more wells are abandoned and sealed. With respect to the previous findings (Vielstädte et al., 2017; Böttner et al., 2020) this raises the questions:

- **if and how frequent gas release occurs at or in the vicinity of (abandoned) wells in the Dutch sector of the North Sea;**
- **if the gas release is caused by the previous drilling and/or inappropriate sealing attempts.**

Furthermore, leaking offshore wells, may form an anthropogenic analogue to natural cold seeps. At cold seeps, methane migrates upwards through cracks and fissures in the sea bed and may be released as dissolved or free gas into the water column (James et al., 2016). Cold seeps are thus methane hotspot point sources and they occur frequently along shelf seas across the globe (Steinle et al., 2015), promoting methane transport to the atmosphere (McGinnis et al., 2006; Deimling et al., 2011). Nevertheless, a substantial amount of the water column methane content at cold seeps is consumed by aerobic methane oxidizing bacteria (MOB) that mediate the aerobic oxidation of methane (MOx; Reeburgh 2007):

-

$$\mathrm{CH_4 + 2O_2 \rightarrow CO_2 + H_2O} \qquad \text{(equation 1)}$$

This raises a further question:

- **if and how much of the released CH_4 is microbially consumed in the water column and how much is ultimately released to the atmosphere.**

With these questions in mind, NIOZ & TNO have been commissioned by SodM to investigate CH_4 dynamics at abandoned wells in the Dutch North Sea. In the first phase of this project, a first research expedition with R/V Pelagia was carried out in summer 2022 (June 2^{nd} to 22^{nd} (cruise PE-503). During this cruise, around 50 well locations were investigated for leakage and ranked for further in-depth investigation. These investigations are aimed to take place during well mixed and fully stratified water column conditions, as this can severely influence methane release to the atmosphere (Steinle et al., 2016). The present cruise, PE-525 was conducted during fully mixed and quite stormy conditions.

During cruise PE-525, we investigated methane dynamics using a variety of different sampling and investigation tools. Video investigation of seepage was conducted with a Remotely Operated Vehicle (ROV Panther, Saab), which was also used to collect gas samples directly and to direct a hose that was lowered form the deck (termed 'SLURF 2.0') to pump water from flare locations to the ship's labs for subsequent analysis. Discrete sediment and water column samples were recovered using a box-corer and CTD water sampler, respectively. Also, the ship's underway systems was used to monitor gas anomalies. Surface water gas exchange was measured with a floating chamber and atmospheric gases were sampled from an inlet at the front mast.

Many observations were conducted with temporal replication (for example repeated CTD casts were carried out at one location over multiple time periods of 8-12h). This was done to account for the high variability of the North Sea system parts of which are likely related to tides.

In addition to research directly surrounding methane, we also capitalised on the sampling opportunity and analyses the carbonate system of sea water. This is determined by the amount of CO_2 added as well as the sea waters pH and alkalinity, which determine the speciation of DIC. CO_2 may leak together with methane from the seafloor; hence methane/CO_2 seepage may directly affect the carbonate system. Finally, we also collected sea water samples to determine the potential for microbial plastic degradation.

Bibliography

Böttner, C., Haeckel, M., Schmidt, M., Berndt, C., Vielstädte, L., Kutsch, J.A., Karstens, J., Weiß, T., 2020. Greenhouse gas emissions from marine decommissioned hydrocarbon wells: leakage detection, monitoring and mitigation strategies. International Journal of Greenhouse Gas Control 100, 103119.

Etminan, M., Myhre, G., Highwood, E.J., Shine, K.P., 2016. Radiative forcing of carbon dioxide, methane, and nitrous oxide: A significant revision of the methane radiative forcing. Geophysical Research Letters 43, 12,614-12,623.

IPCC, 2021. Climate Change 2021: The Physical Science Basis. Contribution of Working Group I to the Sixth Assessment Report of the Intergovernmental Panel on Climate Change, Chemistry International. Cambridge University Press, Cambridge, United Kingdom and New York, NY, USA. doi:10.1515/ci-2021-0407

James, R.H., Bousquet, P., Bussmann, I., Haeckel, M., Kipfer, R., Leifer, I., Niemann, H., Ostrovsky, I., Piskozub, J., Rehder, G., Treude, T., Vielstädte, L., Greinert, J., 2016. Effects of climate change on methane emissions from seafloor sediments in the Arctic Ocean: A review. Limnology and Oceanography 61, S283–S299.

McGinnis, D.F., Greinert, J., Artemov, Y., Beaubien, S.E., Wuest, A., 2006. Fate of rising methane bubbles in stratified waters: How much methane reaches the atmosphere? J. Geophys. Res.-Oceans 111, 15.

Nisbet, E.G., Manning, M.R., Dlugokencky, E.J., Fisher, R.E., Lowry, D., Michel, S.E., Myhre, C.L., Platt, S.M., Allen, G., Bousquet, P., Brownlow, R., Cain, M., France, J.L., Hermansen, O., Hossaini, R., Jones, A.E., Levin, I., Manning, A.C., Myhre, G., Pyle, J.A., Vaughn, B.H., Warwick, N.J., White, J.W.C., 2019. Very Strong Atmospheric Methane Growth in the 4 Years 2014–2017: Implications for the Paris Agreement. Global Biogeochemical Cycles 33, 318–342.

Reeburgh, W.S., 2007. Oceanic methane biogeochemistry. Chemical Reviews 107, 486–513.

Saunois, M., Stavert, A.R., Poulter, B., Bousquet, P., Canadell, J.G., Jackson, R.B., Raymond, P.A., Dlugokencky, E.J., Houweling, S., Patra, P.K., Ciais, P., Arora, V.K., Bastviken, D., Bergamaschi, P., Blake, D.R., Brailsford, G., Bruhwiler, L., Carlson, K.M., Carrol, M., Castaldi, S., Chandra, N., Crevoisier, C., Crill, P.M., Covey, K., Curry, C.L., Etiope, G., Frankenberg, C., Gedney, N., Hegglin, M.I., Höglund-Isaksson, L., Hugelius, G., Ishizawa, M., Ito, A., Janssens-Maenhout, G., Jensen, K.M., Joos, F., Kleinen, T., Krummel, P.B., Langenfelds, R.L., Laruelle, G.G., Liu, L., Machida, T., Maksyutov, S., McDonald, K.C., McNorton, J., Miller, P.A., Melton, J.R., Morino, I., Müller, J., Murguia-Flores, F., Naik, V., Niwa, Y., Noce, S., O'Doherty, S., Parker, R.J., Peng, C., Peng, S., Peters, G.P., Prigent, C., Prinn, R., Ramonet, M., Regnier, P., Riley, W.J., Rosentreter, J.A., Segers, A., Simpson, I.J., Shi, H., Smith, S.J., Steele, L.P., Thornton, B.F., Tian, H., Tohjima, Y., Tubiello, F.N., Tsuruta, A., Viovy, N., Voulgarakis, A., Weber, T.S., Weele, M. van, Werf, G.R. van der, Weiss, R.F., Worthy, D., Wunch, D., Yin, Y., Yoshida, Y., Zhang, W., Zhang, Z., Zhao, Y., Zheng, B., Zhu, Qing, Zhu, Qiuan, Zhuang, Q., 2020. The Global Methane Budget 2000–2017. Earth System Science Data 12, 1561–1623.

Schneider von Deimling, Rehder, G., Greinert, J., McGinnnis, D.F., Boetius, A., Linke, P., 2011. Quantification of seep-related methane gas emissions at Tommeliten, North Sea. Continental Shelf Research 31, 867–878.

Steinle, L., Graves, C.A., Treude, T., Ferre, B., Biastoch, A., Bussmann, I., Berndt, C., Krastel, S., James, R.H., Behrens, E., Boning, C.W., Greinert, J., Sapart, C.-J., Scheinert, M., Sommer, S., Lehmann, M.F., Niemann, H., 2015. Water column methanotrophy controlled by a rapid oceanographic switch. Nature Geoscience 8, 378–382.

Steinle, L., Schmidt, M., Bryant, L., Haeckel, M., Linke, P., Sommer, S., Zopfi, J., Lehmann, M.F., Treude, T., Niemannn, H., 2016. Linked sediment and water-column methanotrophy at a man-made gas blowout in the North Sea: Implications for methane budgeting in seasonally stratified shallow seas. Limnology and Oceanography 61, 367–386.

Vielstädte, L., Haeckel, M., Karstens, J., Linke, P., Schmidt, M., Steinle, L., Wallmann, K., 2017. Shallow Gas Migration along Hydrocarbon Wells–An Unconsidered, Anthropogenic Source of Biogenic Methane in the North Sea. Environmental Science & Technology 51, 10262–10268.

Weber, T., Wiseman, N.A., Kock, A., 2019. Global ocean methane emissions dominated by shallow coastal waters. Nature Communications 10, 4584.

1. Geographical area

Helge Niemann, Chief Scientist

Al sampling during PE-525 was conducted in the North Sea, S of the Doggerbank within the EEZ of the Netherlands (Fig. 1-1). This region features several thermogenic gas fields but also pockets of shallow gas and gas is exploited from numerous wells (www.nlog.nl). Water depth in this area is mostly 30-45 m. In total, we conducted 88 single stations at three main areas, A15-03, B17-4 and B17-5. Sonar and ROV observations at locations A15-03 and B17-5 revealed ~3-5 individual bubble streams directly above the location of the well head, while B17-4 featured many more individual bubble streams (~10-20) that are ~200 m to the S of the well head. A complete station list is presented in the appendix.

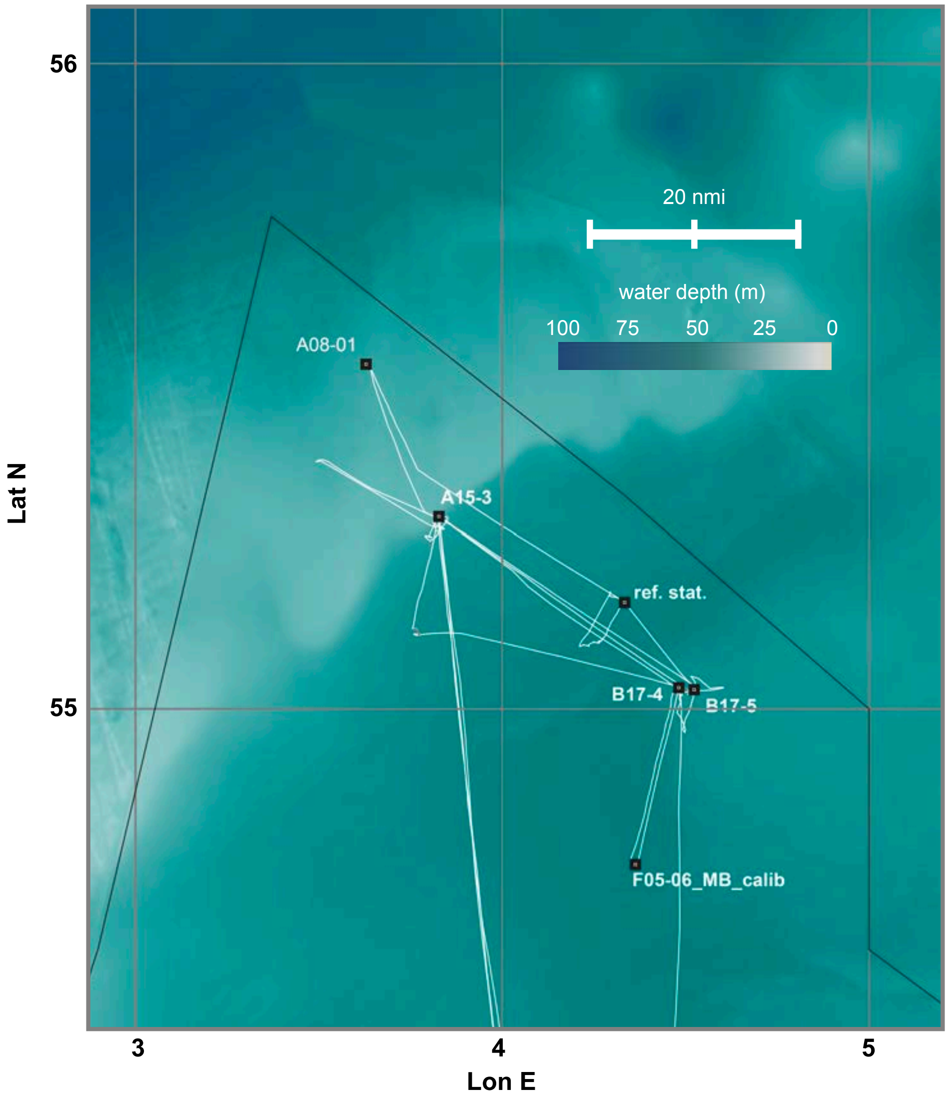

Figure 1-1. Area of investigation during cruise PE-527. Well locations A15-3, B17-4 and B17-5 were investigated in detailed with temporally replicated sampling for CH_4-realted parameters, ROV and Lander deployment. The cruise track is indicated as a white line, sampling stations as black squares.

2. Methane

2.1 Dissolved methane

2.1.1 Discrete water samples

Annalisa Delre

We performed conductivity-temperature-depth (CTD) casts every 2 hours with discrete water sampling over longer time periods. Typically, this comprised uninterrupted time periods of 12h during the day, interrupted by nighttime. In total, each station was thus monitored for a time period of 20 h. To obtain a higher resolution of the dissolved methane in the water column, we decided to collect distinct samples at every 5m (from bottom to surface).
Dissolved methane concentrations were determined using a headspace (HS) technique (Green, 2005). As soon as CTD was in the deck, 260 ml glass serum bottles were filled in triplicates from the Niskin bottles, closed with black-butyl rubber stoppers (Rubber B.V., the Netherlands) and crimped top-sealed. Subsequently, 10ml N_2 was added to create a headspace and we fixed the sample with 5ml NaOH solution (25% w/v). The methane concentrations in the headspace will be measured in our home laboratory with a gas-chromatograph (Thermo Scientific FOCUS GC equipped with a Restek stainless steel column HayeSep-Q, 80/100, General configuration (length 2 m, 2 mm i.d., 1/8 in. o.d.) with flame ionization detection.

2.1.2 In situ measurements

Annalisa Delre

Along with the standard method consisting of sampling with Niskin bottles, a Methane Sensor Type LMS (Franatech GmbH, Germany, Figure 2.1.2-1a) was used to measure dissolved methane concentration in the water column. The detection principle of this device is based on laser absorptiometry. Water is pumped across the laser cavities membrane with a Seabird 5M Titanium pump. The dissolved methane in the water diffuses through a silicon-rubber membrane into the measuring chamber. Absorption of laser light was then proportional to the mixing ratio of methane in the instrument's measuring chamber, which was in equilibrium with dissolved methane in the sea water. With the aid of a factory calibration, the mixing ratio in the cavity was corrected for the inertia of the silicon membrane, allowing to calculate water column methane concentration (Wiesenburg et al., 1979). The sensor was installed in the frame of the CTD carousel and measured during each cast. A second sensor was also installed on the lander frame (see respective section in the cruise report).

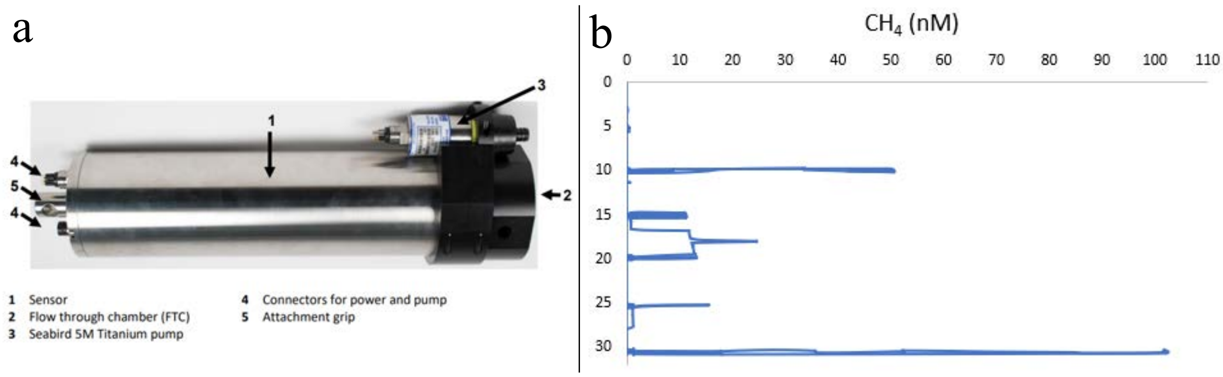

Figure 2.1.2-1. **a)** The Methane Sensor. **b)** Example of water column profile at A15-03, showing the dissolved methane concentration in nM.

Bibliography

Green, J. D.: Headspace analysis Static, in: Encyclopedia of Analytical Science (Second Edition), edited by: Worsfold, P., Townshend, A., and Poole, C., Elsevier, Oxford, 229–236, https://doi.org/10.1016/B0-12-369397-7/00254-5, 2005.

2.1.3 Online measurements of methane in the water phase

Ilona Velzeboer

Equipment

Laser spectrometer	*Tunable Infrared Laser Direct Absorption Spectroscopy; TILDAS; Aerodyne Research Inc., Billerica,UA*
Gas analyses	*Picarro G2401: Picarro, Inc., Santa Clara, USA*

To measure CH_4, C_2H_6, N_2O, CO_2 and CO, a laser spectrometer (Tunable Infrared Laser Direct Absorption Spectroscopy; TILDAS; Aerodyne Research Inc., Billerica, USA) was used. This instrument contains a quantum cascade laser (QCL) and an interband cascade laser (ICL) and can simultaneously measure CH_4, C_2H_6, N_2O, CO_2 and CO.

For measurements of the concentration and composition of gas in the water column, measurements were made with the help of the laser spectrometer on: 1) deep water that was pumped up via a weighted hose ("SLURF") from a few meters above the seabed (**Error! Reference source not found.**a) or 2) surface water of 4 m depth which was taken in at the bow of RV Pelagia via the Aquaflow system of the ship or 3) via the improved SLURF system ("SLURF 2.0"), where a funnel was attached to the hose, which can be placed above a bubble plume with a ROV (**Error! Reference source not found.**.1.3-1b). The funnel was made by Roel Bakker (senior instrument maker; NIOZ). Besides that, it also has an inlet for a controlled release of N_2O into the funnel, to be able to quantify CH_4 coming from the bubble plumes.

The SLURF was deployed from midship starboard side, taped to a steel cable with depressor weight that was lowered via the starboard A-frame (**Error! Reference source not found.**-1c). The SLURF 2.0 was also deployed from midship starboard side, but lowered by hand to where the ROV can take over the funnel. The water from both sources flowed through a few meters of hose to a temperature-controlled lab container placed on the winch deck. The inflow of water from one or the other source used for the laser spectrometer measurements was controlled by means of a valve system.

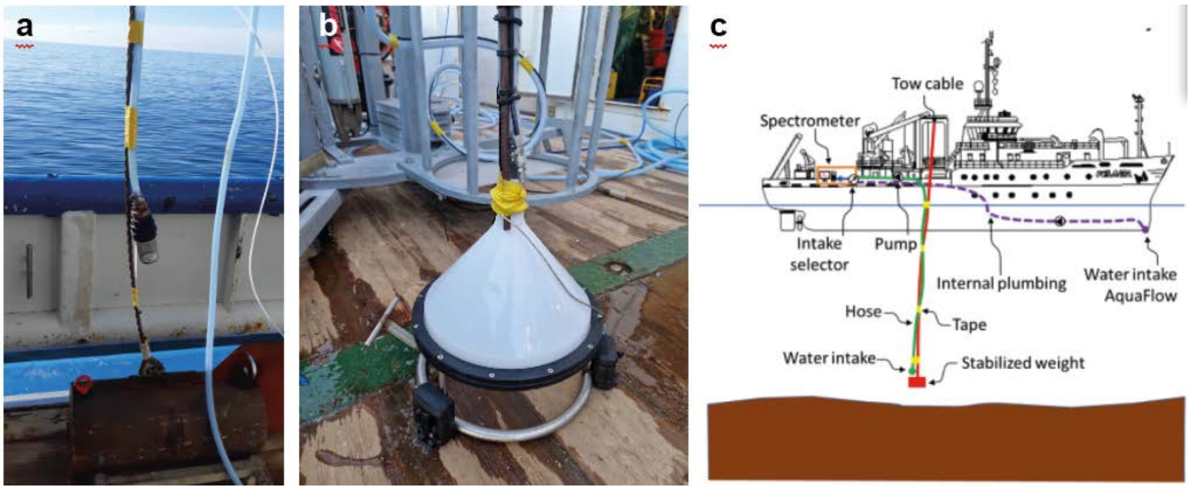

Figure 2.1.3-1. **a)** The lower end of the water intake hose (SLURF), attached to steel cable and depressor weight with stabilizing fin. **b)** The SLURF 2.0 is the improved version of the SLURF. Here a funnel is attached to the hose and has an inlet for a tracer release. On the left side, a grip is shown, that the ROV can use to place the funnel on top of a bubble plume. **c)** Schematic diagram of the setup of the deep water intake hose "SLURF" and the Aquaflow system for the analysis of gases with the laser spectrometer

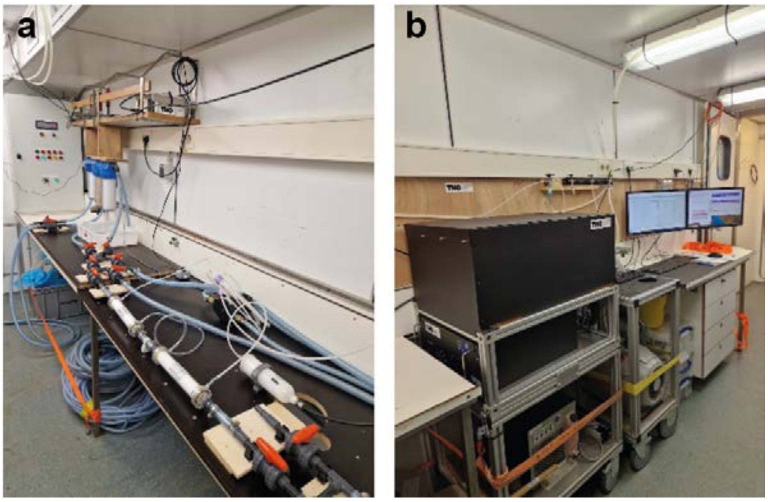

Figure 2.1.3-2. **a)** The "water part" in the container, showing the inlet, the filter system and the membrane set-up. **b)** The "air part" in the container, showing the laser spectrometer and the monitors, to directly see the measured concentrations.

The technique to extract gas from the water phase was performed by using two membranes in series (3M-Liqui-Cel, MM Series; 3M Nederland B.V., Delft). The 3M membrane is able to extract trace gases from the water phase, to make plumes of methane directly visible. Water flows through the two membranes (3M), placed in series, where the air flows in opposite directions, to extract the gases from the water phase. This then goes via a Permapure system to dry the air directly to the laser spectrometer.

A picture of the water part, with the 3M Liqui-Cel membranes is shown in **Error! Reference source not found.**, and a picture of the air part, with the laser spectrometer is shown **Error! Reference source not found.**. When the ROV is in the water, the SLURF 2.0 with the funnel can be used. When meteorological conditions were not suitable for ROV deployment, the SLURF with the weight was used for water sampling. When there was no SLURF sampling, like during transits or CTD sampling, the surface water collected with RV Pelagia's Aquaflow system was analyzed. Or, if the wave height allows, floating chamber measurements were performed, using the same laser spectrometer measurements (more information about the floating chamber can be found in 2.3.1).

One SLURF 2.0 measurement was performed with the ROV at station A15-03, just above a bubble plume (**Error! Reference source not found.**). High concentrations were measured, samples for CH_4 measurements with GC-MS were taken before and after the membranes, to compare concentrations and to check on the efficiency of the membranes. Unfortunately, the funnel broke from the hose. The ROV was still able to place the funnel with the hose close to the bubble plumes, but the N_2O tracer release did not work in this case.
A second SLURF 2.0 measurement was performed with the ROV at station B17-04. This locations was deeper, so the funnel was places higher in the water column. And because of less visibility at this location, the right place to catch the bubbles several meters above the plume was difficult to find.

SLURF measurements were performed when the ROV was not able to go into the water, because of the weather conditions (example of preliminary results in **Error! Reference source not found.**). These measurements were performed at 24, 26, 27 and 28 October.

Aquaflow measurements were performed from 22 October continuously if no SLURF or floating chamber measurements were done (example of preliminary results in **Error! Reference source not found.**).

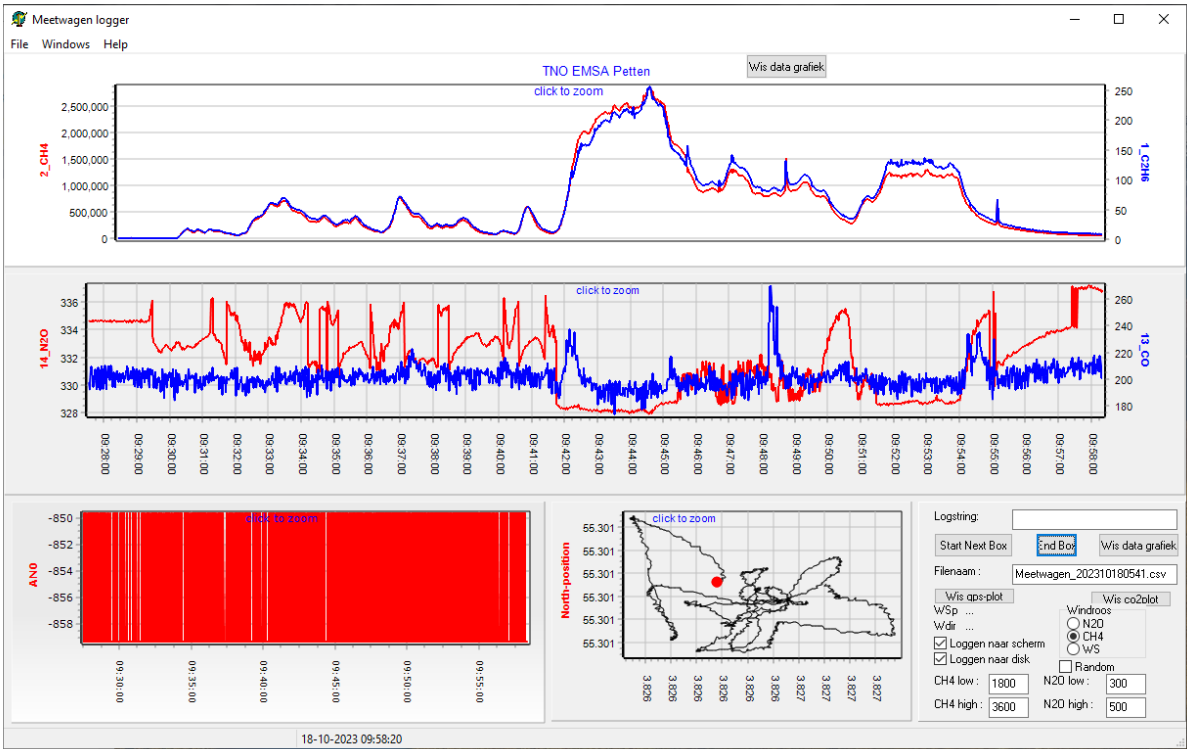

Figure 2.1.3-3. Example of SLURF 2.0 measurements at A15-03 just above the bubble plume, showing CH_4 and C_2H_6. CH_4 concentration wend up to 2500 ppm, with is above the upper limit of detection (oversaturation of the measurement system).

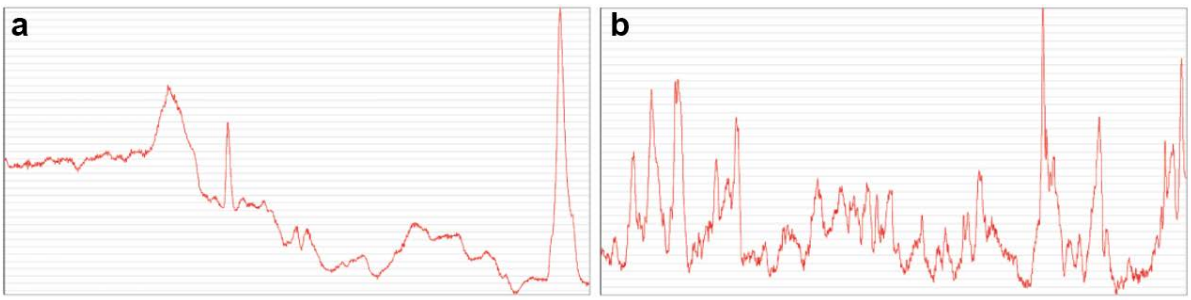

Figure 2.1.3-4. **a)** Example of CH_4 bubbles measured via the SLURF at B17-04. The measurement time was 30 min and concentration went up to 160 ppb (24-10-2023 09:23-09:53 UTC). **b)** Example of CH_4 bubbles measured via the aquaflow system at B17-04. The measurement time was 30 min and concentrations went up to 50 ppb (23-10-2023 07:53-08:23 UTC), but clearly visible.

2.1.4 Methane in sediments

Annalisa Delre

Sediments samples were collected using a box corer and subsampled with 3 small push cores (diameter = 7 cm). From each push core, we collected 5ml of sediment every 2cm that was added to 60ml glass bottles containing 30ml of a saturated NaCl brine solution. The bottles were immediately sealed with butyl rubber stoppers. The methane concentration in the sediments will be measured in the laboratory similar to water column samples.

2.2 Methane consumption

2.2.1 Methane oxidation rates

Annalisa Delre

Methane oxidation rates (MOx) in the water column were determined by ex-situ incubation with trace amounts of ^{3}H-labelled methane as describe previously (Niemann et al., 2015). Aliquots from the Niskin bottle were filled in 20ml glass vials in quadruplicates, sealed with grey-bromobutyl stopper that are known to not hamper methanotrophic activity. These samples were then amended with 10ul of $^3H\text{-}CH_4$ (American Rabiolabeled Chemicals, USA) and incubated for ~72h at situ temperature in the dark. The activities of residual C^3H_4 and the product of methane oxidation (^3H_2O) were measured by liquid scintillation counting. The First-order rate constant (*k*) was then determined from the fractional turnover of the added tracer (Reeburgh, 2007):

$$k = \frac{^3\mathrm{H_2O}}{^3\mathrm{H_2O} + \mathrm{C^3H_4}} \times \frac{1}{\mathrm{t}} \qquad \text{(equation 2.2.1-1)}$$

where *t* is incubation time in days. *k* was corrected for tracer turnover in killed controls (k_{KC}, fixed with 10ul $HgCl_2$ directly after sampling) and multiplied with methane concentrations [CH_4], resulting in MOx:

$$\mathrm{MOx} = (k - k_{\mathrm{KC}}) \times [\mathrm{CH_4}] \qquad \text{(equation 2.2.1-2)}$$

2.2.2 Methane Oxidizing Bacteria

Annalisa Delre

Water aliquots (2l) for identification and quantification of methane oxidizing bacteria (MOB) were collected in triplicate from surface and bottom waters and stored in 2l glass bottles (rinsed three times before filling). The water was then filtered through glass fibre filters (pore size 0.3 µm, diameter 47 mm, ADVANTEC®, GF-75) placed on Swin-Lok filter holder (Whatman®) by using a peristaltic pumps. The filters were stored at -80 °C for further analysis (DNA extraction/sequencing) at NIOZ.

Bibliography

Niemann, H., Steinle, L., Blees, J., Bussmann, I., Treude, T., Krause, S., Elvert, M., and Lehmann, M. F.: Toxic effects of lab-grade butyl rubber stoppers on aerobic methane oxidation, Limnol. Oceanogr.-Meth., 13, 40–52, https://doi.org/10.1002/lom3.10005, 2015.

Reeburgh, W. S.: Oceanic Methane Biogeochemistry, Chem. Rev., 107, 486–513, https://doi.org/10.1021/cr050362v, 2007.

Wiesenburg, D. A., & Guinasso Jr, N. L. (1979). Equilibrium solubilities of methane, carbon monoxide, and hydrogen in water and sea water. Journal of chemical and engineering data, 24(4), 356-360.

2.3 Sea-atmosphere fluxes of methane

2.3.1 Floating chamber

Ilona Velzeboer

Figure 2.3.1-1. The Floating chamber (DONUT), left: floating chamber on deck, right: floating chamber deployed in the water.

A special floating chamber, suitable for offshore measurements is designed by Dave Huijsman (senior sea technician; NIOZ) (**Error! Reference source not found.**). The chamber has a diameter of 60 cm. the height of the chamber is adjustable, but for this cruise set to middle setting, resulting in a height of 39 cm. The used chamber settings had a total air volume of 139 L (because of the waves, this could be a bit variable, but the height cancels out in the final calculation of the flux). A ½" tubing is used to go from the container to the floating chamber and back (in total 60 m), to have a closed loop.

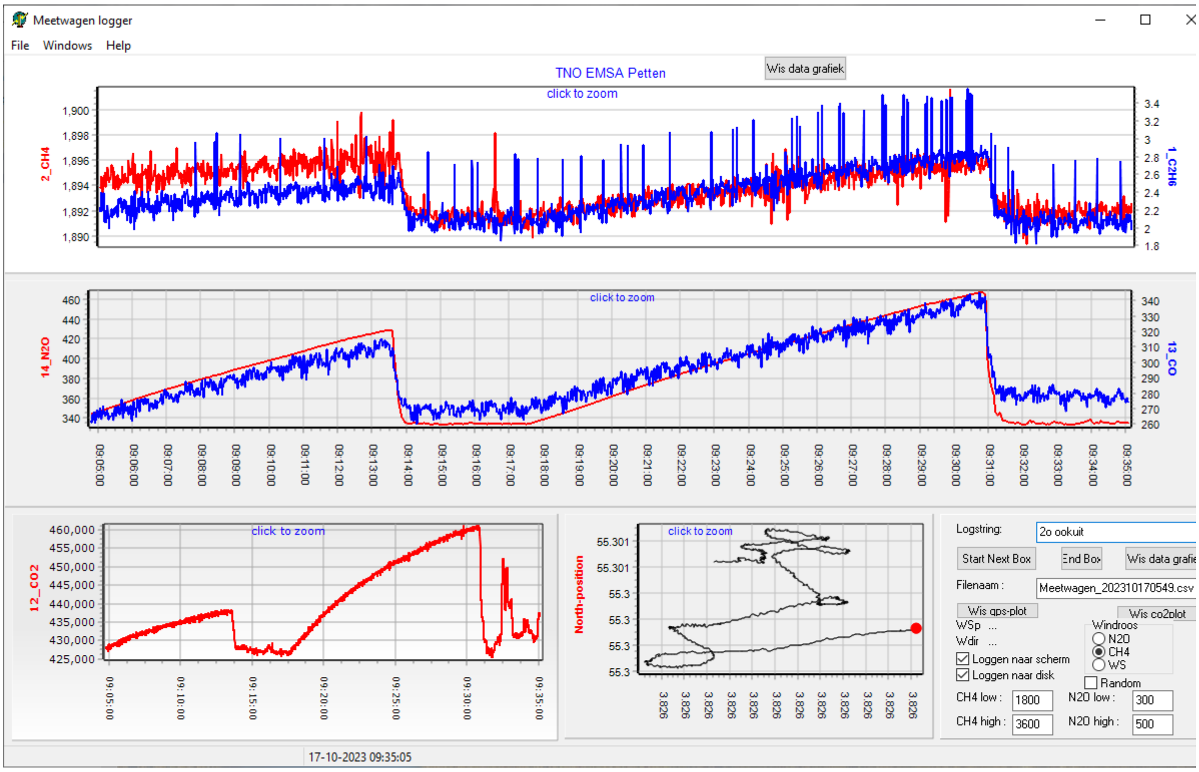

Figure 2.3.1-2. Preliminary results of floating chamber measurement at A15-03. In this example no CH_4 bubbles were measured

Compressed air with an added amount of N_2O (8 ppm), was added to the return line with a controlled flow. This was done to be able to quantify the flux of CH_4 coming from the water phase. The air inside the chamber is mixed by a propeller driven by a pneumatic pistol. During the last deployment, the propeller got lost, but Dave fixed a new one!
The floating chamber was deployed at 16 and 17 October at A15-03 (example in **Error! Reference source not found.**), 23 October at B17-04 and 26 October at B17-05. When the waves are getting too high, the floating chamber gets partly out of the water and is not able to measure properly anymore.

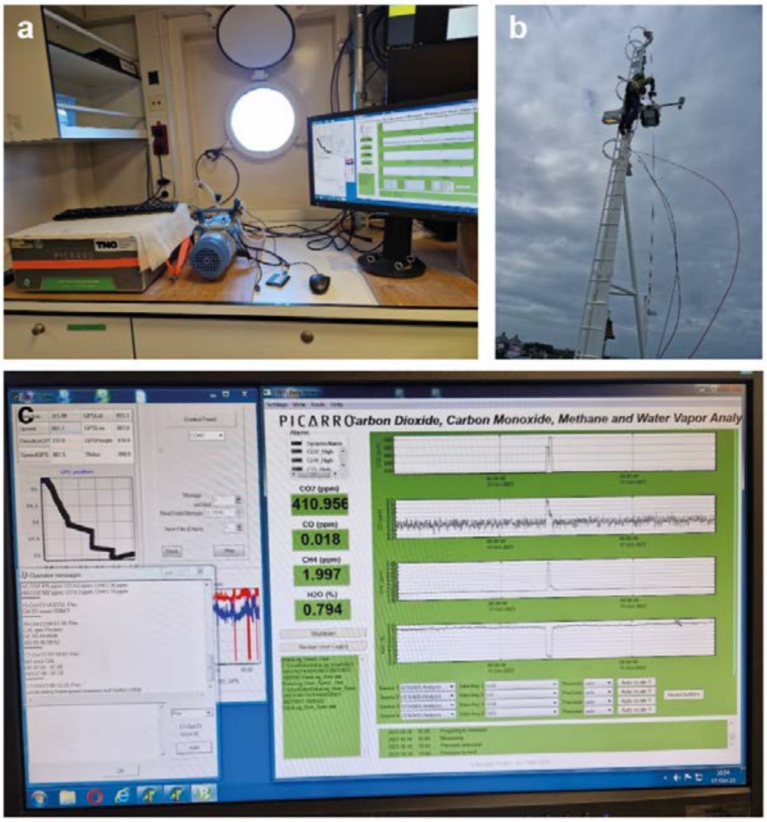

Figure 2.3.2-1. **a)** the Picarro set-up in the dry lab at RV Pelagia. b) Installation of the inlet and 2D sonic anemometer at the foremast for continuous atmospheric measurements. **c)** image of resulting measurements. On the left, data from the GPS corrected 2D sonic anemometer is recorded, on the right, data from the Picarro is shown, CO_2, CO, CH_4 and H_2O. The plume in the middle is the measured calibration gas.

2.3.2 Atmospheric measurements

Ilona Velzeboer

In addition to water sampling for analysis of gases, air was continuously taken in at the foremast of the ship at approximately 10 m above sea surface and led via tubing to the wet lab for analysis of atmospheric CH_4, CO_2 and CO with a Picarro G2401 gas concentration analyzer (Picarro, Inc., Santa Clara, USA) (**Error! Reference source not found.**). Next to the inlet, also a GPS corrected 2D sonic anemometer was placed (**Error! Reference source not found.**). The 64PE525 North Sea Methane Expedition measurements started on 14 October, when installing all instruments onboard and stopped on 1 November, when entering the NIOZ harbour. Continuous measurements took place in between, an example of the continuous measurements is shown in **Error! Reference source not found.**.

2.4 Echosounder-based detection of bubbles

Noortje Versteijlen, Henk de Haas

A full list of all multibeam (EM302 or EM2040) and water column echo sounder (EK80) flare surveys can be found in the appendix.

2.4.1 Ships mounted MB, single beam

In combination with a multibeam echo sounder (Kongsberg EM302 or EM2040SRX) a Kongsberg EK80 Scientific Echo Sounder system was used to study gas flares in the water column. During a period of several hours one EK80 line and one multibeam line were recorded each hour in an area of known gas flares in order to study any possible temporal (tide related) changes in gas flux. Recording of the instrument was done separately to avoid interference of one tool on to the other. The sailing speed was aimed to be 2 knots to allow sufficient data points to be recorded within the water column needed for proper statistical analyses of the reflection strength (enough data points per 3D water column grid cell in). Each individual survey was planned to be carried out along the same line, but because of strong and variable wind, wave and current conditions during a survey the line orientation regularly had to altered to be able to keep following the track at the required low sailing speed.

2.4.1.1 Single beam echo sounder

The EK80 is a system consisting of one or multiple transducers with centre frequencies ranging from 18 to 333 kHz. For this study a mobile system, installed on the port side measurement pole of the vessel, was used consisting of a wide band transceiver (WBT mini) and two transducers with nominal frequencies of 70 and 200 kHz (Simrad ES70-7C and ES200-7C respectively). Due to installation issues, during the earlier parts of the cruise only the 200 kHz transducer was used.
The ES70-7C is a split beam transducer with a bandwidth of 45-90 kHz and a circular beamwidth of 7 degrees. The ES200-7C also is a 7 degrees split beam transducer. The bandwidth for this device ranges from 160 to 260 kHz.
Position and motion data is stored within the datafile. This information is supplied by the Seapath380/MRU 5+ ships attitude system. The position of the transducers on the pole relative to the GNSS antenna and MRU5+ is included in the final positioning of the data.
Data was recorded using the matching Kongsberg EK80 software. The data was stored in raw format.

2.4.1.2 Multibeam echo sounders

EM2040SRX

Initially all surveys were planned to be carried out with a high resolution Konsgberg EM2040SRX mobile multibeam echosounder mounted on the ships port side measuring pole. As a result of technical issues with the connected Seapath380 ships attitude system the EM2040SRX could not be used during several of the surveys (see the overview table to see which surveys). After consulation with the manufacturer it was concluded that the problems were caused by the software present in the Seapth380 processing unit resulting in the use of wrong communication port settings by this system on its turn resulting in problems with the pinging of the multibeam (no pinging, while internally the system reported it was pinging). After several days of consultations with the manufacturer these issues were overcome. However this resulted in a way of attitude data transmission (delayed transmission) from the Seapath to the multibeam that was not optimal for bathymetric surveys, but would have hardly any effect on the quality of the water column data. Gathering the latter being the main reason for the surveys, it was decided to accept this solution. During the surveys were the EM2040SRX could not be used the ship mounted medium-deepwater EM302 multibeam was used.

Because of operation technical reasons this system was fitted with its own Seapath ships attitude and navigation system and a MRU5+ mounted on the EM2040 transducer pod. The Seapath GNSS antennes were mounted on a separate frame installed on the bridge of the vessel. To ensure high accurate navigation allowing a data quality fitting the EM2040 specifications a Konsgberg 3710 DGNSS receiver was used in combination with a Fugro MarineStar subscription.

The EM2040SRX is a high resolution 200-700 kHz shallow water multibeam. Experience during the 2022 cruise for this project has shown that running it at a frequency of 400 kHz gives the best possible results. Therefore also this year surveys were carried out using 400 kHz. The beam opening angle at this frequency is 0.4°x0.7° for the transmitter and receiver beam angle respectively. The swath opening angle was fixed at 60° port side and starboard side. Beam stabilisation is similar to the EM302.

The sound velocity sensor mounted on the transducer pod turned out to be not working. The sound velocity near the transducers was taken from the sound velocity profile determined by the CTD casts taken during the cruise.

Because of the problems with the system occurring at the start of the cruise, time lost due to bad weather and the tight sampling program, there was no time to calibrate the system before the surveys took place. The raw data is therefore effected by artefacts (especially a pitch error is clearly noticable in the bathymetry). A EM2040 offset calibration was carried out at the end of the cruise. Therefore the resulting offset correction have to be applied to the raw data post cruise.

EM302

After the failure of the EM2040SRX, surveys were continued using the ships EM302 medium-deep water multibeam echosounder. Since this is a lower frequency system now used in shallow water, the data is not of as good quality as would have been possible with the EM2040.

The Kongsberg EM 302 multibeam echosounder presently installed on board the Pelagia is a 30 kHz echo sounder with a one degree opening angle for the transmitter and a two degree angle for the receiver. It uses 288 beams with 2-3 depth measurements per beam. The system is equipped with a dual swath, resulting in a maximum number of depth measurements of 864 per ping. The maximum swath opening angle is 150°. During the described surveys the opening angle was fixed at 120°. The transmit fan can be split into at maximum 9 individual sectors that can be steered independently to compensate for ships roll, pitch and yaw to get a best fit of the ensonified line perpendicular to the ships track and thus a uniform coverage of the sea bed. The transducers are mounted in a gondola which is placed at the port site of the vessel at about one quarter to one third of the ships length from the bow. The motion of the vessel is registered by the same Kongsberg MRU-5 motion reference unit as mentioned above. Ships position and heading is determined with two GNSS antennas. The motion and position information is combined in a Seapath 380 ships attitude processing unit and send to the Transmit and Receiver Unit (TRU). The system is synchronized by means of a 1 pulse per second (1PPS) signal produced by the Seapath 380 which is send to the TRU. The data from the receiver transducer and the ships attitude are sent through an ethernet connection to the acquisition computer. Data acquisition is done using the Kongsberg SIS (Seafloor Information System) software. The sound velocity profile is calculated from salinity, pressure and temperature data recorded by a Seabird CTD system. During the cruise the Reson SVP 70 sound velocity probe that is normally mounted on the gondola containing the transducers and measures the sound velocity near the transducers was not available. The near-transducer sound velocity was taken from the calculated velocity profile. The processing PC is connected to a display on the bridge of the Pelagia through a KVM switch and an ethernet connection allowing operation of the system from the bridge if desired. On board the location of flares was determined using Fledermaus MidWater.

2.4.2 ROV mounted ARIS

The ROV was equipped with an ARIS Explorer 3000 imaging sonar (Fig. 2.4.2-1) produced by Sound Metrics. The two main aims of this instrument were 1) detecting the presence of gas seeps and help guiding the ROV towards the seep locations and 2) use the high-resolution images to determine individual bubble size and bubble rates order to quantify the volume of gas being released within a certain time period at these sites.
The ARIS 3000 Explorer is a high resolution acoustic imaging instrument using a frequency of 1.8 MHz in detection mode and 3 MHz when in identification mode. The image is constructed from its 128 individual beams. During the cruise the high resolution 3 MHz identification mode was used. This resulted in high quality `acoustic video' data. Because of the high frequency used, the range of the system is limited to about 5 metres in identification mode. However since the acoustic signals were not hampered by the very high concentration of suspended material in the water column, limiting the optical visibility often to less than the length of the ROV manipulator arm, it was still possible to produce the needed high resolution imagery. An example of the quality of the ARIS data can be seen on the cover of this cruise report, showing a video still of a fish investigating a methane bubble stream at one of the visited seep locations. A further example is shown in Fig. 2.4.2-3

Figure 2.4.2-1 The complete ARIS Explorer 3000 equipment. The underwater transducer unit is shown on the right hand side (size about 30x18x14 cm). Image by Sound Metrics.

When interpreting ARIS images, one has to take into account that the sonar produces a 2 dimensional image of a 3-dimensional world (Fig. 2.4.2-2). In addition to this, because the positioning of the ROV relative to the seep site can be limited due to wave (shallow water and sometimes strong wave action during the cruise, waves can influence conditions at the seabed) and tidal current conditions it was not always possible to have an optimal orientation of the acoustic camera which could result in non-optimal imaging orientations. In addition to this, one has to realise that the `viewing direction' of the camera is not the same as the viewing direction of the observer watching the screen (Fig. 2.4.2-2).

In order to be able to find out whether it would anyway be possible to use the ARIS 3000 for gas seep quantification, before the cruise a test was carried out in the NIOZ test basin on Texel. An ARIS 3000 was placed in the test basin and pressurised air was used to mimic gas seeps. Using this setup it became clear that it should be possible to use the ARIS system for the intended task. But because of image distortion, relatively low resolution imagery compared to optical images and having only a 2-dimansional image available of 3-dimensional bubbles, it would be necessary to take a certain uncertainty and scaling factor into account when the final seep rate calculations will be carried out.

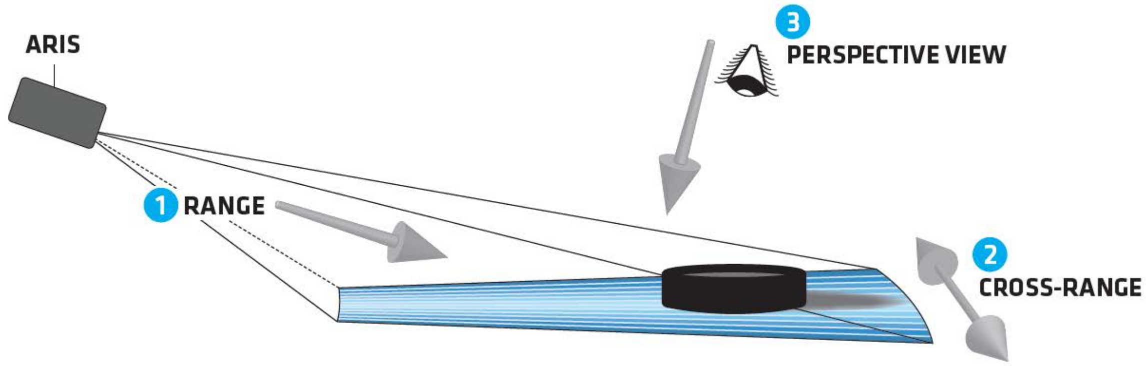

Fig. 2.4.2-2. Image illustrating the viewing direction of the ARIS 3000 and the perspective view of the observer. Image by Sound Metrics.

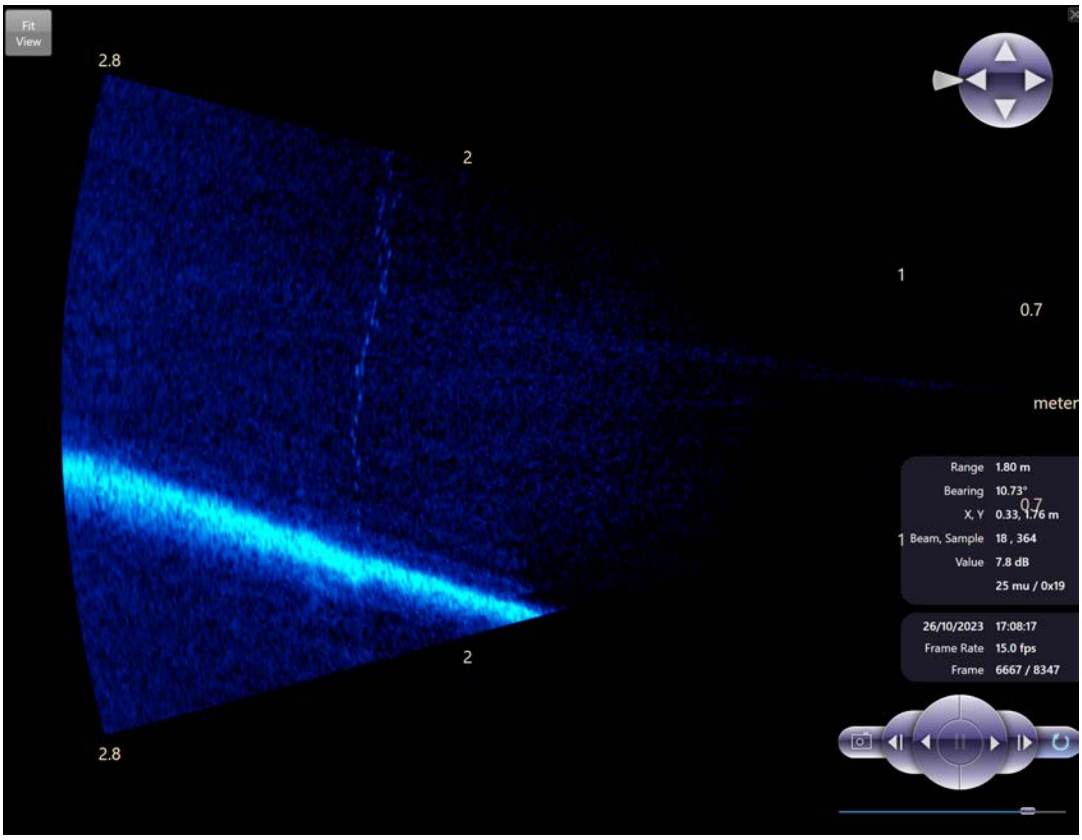

Fig. 2.4.2-3 Screenshot of the ARIS 3000 as an example of the data quality produced by the system. A bubble stream can clearly be observed in the centre of image.

2.5 Albex Lander

Noortje Versteijlen, Henk de Haas

Introduction

An autonomous lander frame was developed by NIOZ that was equipped with multiple sensors and cameras to enable long-term timelapse measurements and recordings. For the PE-525 cruise, the lander was equipped with an HD camera and sensors to measure methane, current, pH, dissolved oxygen and salinity. The HD camera and Methane sensor were powered by a battery-pack that was attached to the lander. The rest of the sensors were powered by internal batteries.

Figure 2.5.-1. The Albex lander on deck

During the PE525 cruise the lander was deployed at three locations, namely near two leaking wells and one natural seepage location. Before lander deployment, the bubble plume locations were determined with the multibeam and single beam echosounder. Based on the plume locations, the lander was deployed as close as possible with respect to the bubble plumes. A big factor in placing the lander was the influence of wind and waves, since it takes several seconds to deploy the lander after the deployment signal was given. Since we encountered high waves and strong winds deployment was challenging. After each deployment of a few days, the lander was retrieved and the data from each sensor and camera was collected.

Measurement equipment and configuration

Tab. 2.5.-1. Equipment mounted to the lander with the used configurations during PE-525.

Equipment	Model	Serial number	Last calibration	Software	Interval
Current	Nortek Aquadopp current profiler	50376-1681	July 2023	Aquapro V20.00.02	5 min
Oxygen	JFE Advantech ARO-USB	0205	New sensor, no calibration done	JFE-Advantec JOGOS V1.05	10 min
pH	AquapHOx-LX	21410016	Before each deployment	PyroWorkbench	30 sec
Methane	Franatech	05-10618	n.a.	Franatech Datalogger Support	30 sec
CTD	Microcat CTD SBE37	5389	05-may-07	Sea Term V1.59	10 min
HD Camera	Rayfin SubC Camera	00111010	n.a.	SubC Rayfin Control V3.4.8	15 min

Current profiler (Aquapro)

The Nortek aquadopp current profiler (Aquapro) measure current speed and direction in multiple layers, or vertical cells, through the water column. The idea of vertical cells is that the currents vary little in the horizontal plane, but may differ more in vertical layers during for instance the tidal cycle. An acoustic Doppler instrument transmits a short pulse of sound ("ping") of constant frequency into the water, listen to its echo and measure the change in pitch or frequency of the echo caused by the doppler effect.
The temperature is measured by a thermistor embedded in the head and reported in degrees Celsius. This information is of vital importance, since the instrument uses the speed of sound to convert time to distance, and the speed of sound depends on temperature. Furthermore, the hydrostatic pressure is measured with the pressure sensor and reports in units of dbar.

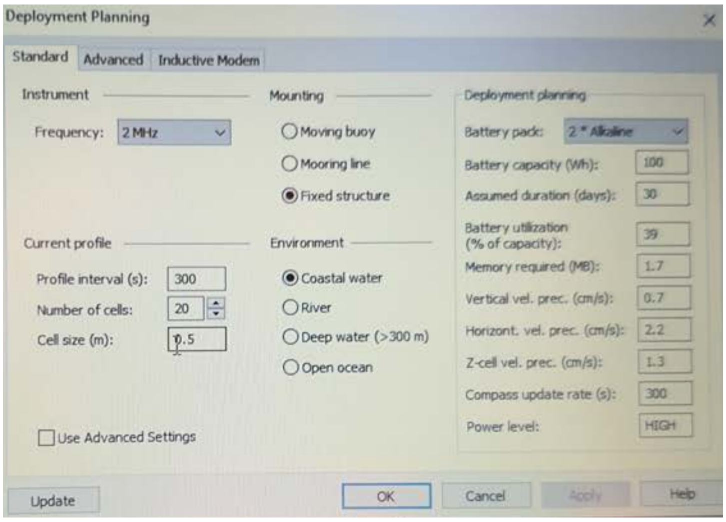

Figure 2.1.-2 Settings of the Aquapro current profiler

During PE-525, the current profiler was mounted on the lander with the transducer head facing upward and level with the top of the frame, so that it has an unobstructed 'view' into the overlying water column. During the deployment of the lander, every 5 minutes the current and direction was measured over 20 cells of each 0.5 m, covering a water column of 10 m. Also, the pressure and temperature at the instrument was measured every 5 minutes.

Oxygen Sensor (Rinko)

The Rinko is a fast-response, high-accuracy and high-resolution dissolved oxygen (DO) sensor with a response time of less than 1 s in air. This enables DO measurements with continuous DO profiling at high speed (~ 0.5 m s^{-1}) and to acquire high resolution DO distributions. The sensor contains an optical window that is coated with photostimulable phosphor. The blue LED pulse from the sensor generates a red phosphorescence pulse, which in turn has an inverse correlation with the oxygen partial pressure in the water. The Rinko also contains a thermistor for measuring water temperature.

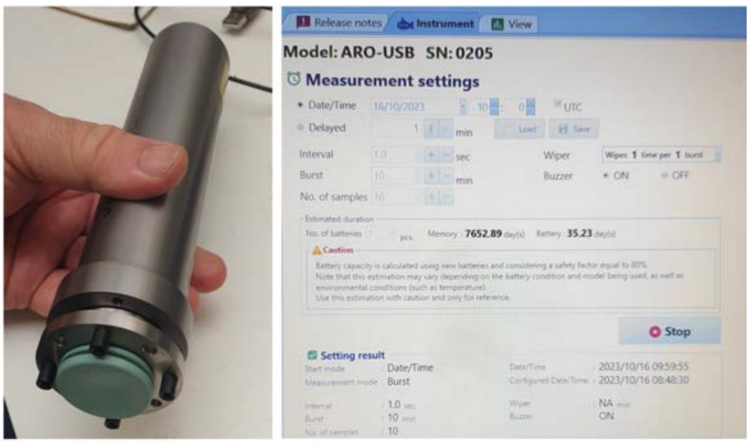

Figure 2.5.-3 Oxygen sensor (Rinko) and deployment planning

During the PE525 expedition, for each lander deployment every 10 minutes a burst of 10 samples was made, with a time interval of 1 sec per sample. Per sample the temperature (°C) and dissolved oxygen (in %, mg/L and µmol/L) was measured.

pH sensor

In order to understand the changes in pH with the tidal cycle in the North Sea, a pH sensor was deployed on the Lander to collect high-resolution continuous pH data. The data collected by this sensor will be combined with other data from the CTD sampling to characterize the carbonate system dynamics in the North Sea.

A Pyroscience pH logger optode was fixed on the Lander in order to record the pH during the deployments that were performed. The sensor was in stand-alone logging mode during the whole process collecting pH data every 30 seconds. The data was retrieved from the sensor once the Lander was back on deck. Before deployment, the sensor was calibrated with pH 2 and pH 11 buffer solutions. Another middle point calibration point was performed with a TRIS solution prepared at NIOZ.

Methane sensor

A sensor based on laser absorption (Franatec LMS) was mounted on Albex. This sensor was the same model as the one mounted on the CTD frame; see chapter 2.2 for specifications.

CTD (MicroCAT)

The SBE 37-SM MicroCAT (CTD) is a sensor that measures water parameters in one location over an extended period to produce a time-series of data. It measures the Conductivity (S/m), Temperature (°C) and pressure (dbar), from which the variable salinity and sound velocity of the seawater can be derived.

Fig 2.5.-4 CTD (MicroCAT)

During the PE525 expedition the MicroCAT was fixed vertically in the top part of the lander. During deployment every 10 minutes the conductivity, temperature and pressure were measured and from which salinity was derived (not sound velocity).

Rayfin SubC Camera

The Rayfin SubC HD camera was used for time lapse recording of digital stills and HD videos with the use of a hibernation feature. The camera runs through a series of commands in a script and then hibernates to use as little power as possible. Then after a pre-set period of time, the hibernation function will power the camera up to run through the script again.

During the PE525 cruise the camera was mounted in the lower part of the frame looking from the side into the open space below the center of the lander. The part of the lander frame in sight of the camera was provided with a scalebar, which enables to roughly scale the bubble sizes in case the methane bubbles were captured by the camera. A LED light was placed vertically above the open space facing downwards to area within viewing range of the camera to lighten the area during the recording of the footage. The script with series of commands was executed, making multiple recordings every 15 minutes. The camera was externally powered by a 24V battery pack and all the recordings were stored in the camera's internal memory.

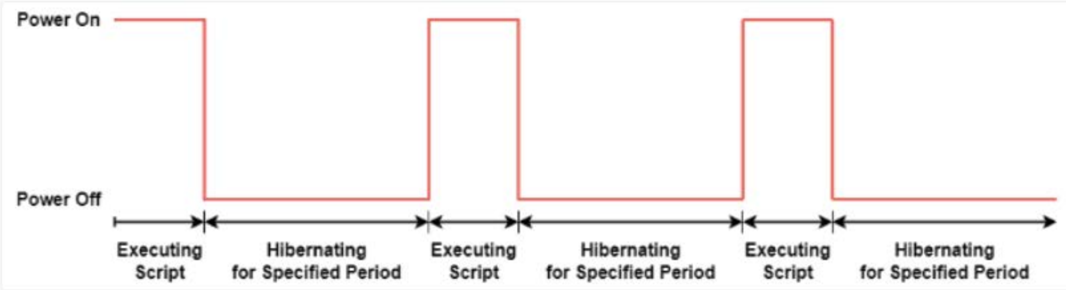

Recordings every 15 minutes with Rayfin SubC HD camera. Timelapse recordings = 15 sec			
Name	**Shutter speed (nanoseconds)**	**ISO**	**recording**
Still_Manual_A	8000000	150	
Still_Manual_B	4000000	200	
Still_Manual_C	2000000	400	
Still_Auto_A	auto	auto	
Still_Auto_B	auto	auto	
Still_Auto_C	Automatic	auto	
Videos_Timelapse	auto	auto	15 sec

Figure 2.5.-5. Oscillation of hibernation and measurement mode of the camera (top). The camera frame with size reference for measurement (left). Camera shutter times are indicated (right).

3. Carbonate system

Yasmina Ourradi

The principal sampling program consisted of full-depth CTD profiles with a rosette equipped with 24 “PRISTINE” ultraclean sampler bottles developed by NIOZ (Rijkenberg et al., 2015). Oxygen, carbonate system (pH, Total Alkalinity, and Dissolved Inorganic Carbon), salinity, nutrients, and carbon isotopes samples were collected by Yasmina Ourradi, Annalisa Delre, Robin Van Dijk, Pepien Rubbens and Jessica Riekenberg. The rosette was equipped with a Temperature-Conductivity-Depth, pH, methane, and dissolved oxygen sensors and their data was fed into the CTD data stream.
For every deployment, pH Total Alkalinity, Dissolved Inorganic Carbon, nutrients, and carbon isotope samples were collected. These parameters were sampled for every depth, while the isotope samples were only sampled at the surface, intermediate and bottom depths. Salinity and Oxygen samples were collected at various depths for selected deployments due to the limited number of bottles.

3.1 Discrete water samples

3.1.1 Dissolved oxygen: oxygen samples were collected once in a ~120 ml glass bottle with Tygon tubing and following the Winkler method. The bottles are filled and overflown with at least three times its volume, it is of great importance that there are no bubbles in the samples. Immediately after filing the bottles, two reagents are added, manganese chloride ($MnCl_2$, 1 ml) and a mix solution of sodium hydroxide and potassium iodide (NaOH/KIO, 2 ml). The glass stoppers are inserted displacing the excess of water. A rubber band is used to tighten the seal and the samples are thoroughly shaken and then shaken again after 15 minutes. The samples are kept in the dark and stored underwater at 25°C before analysis.

3.1.2 Carbonate system: samples for pH, total alkalinity (TA), and dissolved inorganic carbon (DIC) were collected following the best-practice recommendations (Dickson et al., 2007a). The samples were collected with Tygon tubing into 250 ml borosilicate glass bottles. The bottles were rinsed three times, filled from the bottom smoothly, overflown for two times the bottle volume, and sealed with ground glass stoppers.
Once in the laboratory, a headspace in the DIC and TA samples was created by removing 1% of the volume to allow the expansion of the seawater, then the samples were poisoned with a saturated mercury (II) chloride solution (50 µl) to prevent any biological activity. The samples were sealed with greased glass stoppers to prevent gas exchange and secured with tape. Samples were then thoroughly mixed and stored in the dark at 25 °C. Most pH samples were not poisoned with mercury chloride as they were analysed within 12 hours of collection.
In addition, pH, TA, and DIC samples were also collected from the underway system after the end of the daily CTD sampling. Samples were collected at 22:00, 24:00, 03:00, and 06:00 (ship time) to correct the drift of the underway sampling (section 3.3)
The sampling for pH, TA, and DIC should be handled with care because of the CO_2 exchange between the atmosphere and the samples which could compromise measurement.

3.1.3 Stable isotopes of DIC: DIC isotope samples $\delta^{13}C$-DIC were directly collected in 20 ml glass vials then sealed and stored in the fridge until analysis. Samples were only collected at surface (5 m), intermediate (25 m) and bottom (40 m) depths.

3.1.4 Salinity: samples for salinity were collected into 200 ml glass salinity bottles that were rinsed three times before filling. The bottle-necks were first dried in order to prevent salt crystallization, afterwards, the bottles were sealed with plastic inserts and then closed with screw caps. The samples were stored in the lab-container to be analyzed at NIOZ.

3.2 In situ pH measurements

The pH samples were measured during the cruise in the NIOZ container-lab by spectrophotometry using the Agilent Cary 8454 UV-VIS spectrophotometer. The analytical procedure for pH analysis by spectrophotometry is based on Clayton and Byrne (1993) method and following the guide to best practices for ocean CO2 measurement (Dickson et al., 2007).

The samples were transferred into a spectrophotometer glass cell without or as little as possible contact with the atmosphere. Once filled, the cells were closed with stoppers to prevent gas exchange and placed in an aluminium warming box attached to a water bath where the water is circulating and maintaining the temperature at 25± 0.2°C. Afterwards, every cell is placed in the cell holder on the spectrophotometer and a reference spectrum is recorded, then 10 µl of m-Cresol Purple is added to the cell, and up to 5 absorbance spectra are recorded. The resulting absorbances are used to recalculate the pH.

3.3. Continuous flow measurements

During the cruise, an aquaflow system was installed to continuously measure surface seawater pH whenever the aquaflow was operational. However, there was one exception was on November 16th when the system became disconnected. The problem was fixed and was due to a faulty connecting cable.

The pH optode system from Pyroscience was connected to the aquaflow setup. Before the start of measurements, the pH optode underwent calibration using low (pH 2) and high (pH 11) buffers from Pyroscience. In addition, an intermediate middle point calibration was performed by using a pH tris buffer prepared according to the protocol outlined in Paulsen and Dickson (2020).

After the cruise, a drift correction might be applied based on the CTD pH samples and the underway spectrophotometric pH measurements.

Bibliography

Clayton, T. D. and Byrne, R. H.: Spectrophotometric seawater pH measurements: total hydrogen ion concentration scale calibration of m-cresol purple and at-sea results, Deep Sea Research Part I: Oceanographic Research Papers, 40, 2115–2129, https://doi.org/10.1016/0967-0637(93)90048-8, 1993.

Dickson, A. G., Sabine, C. L., and Christian, J. R. (Eds.): SOP 1: Water sampling for the parameters of the oceanic carbon dioxide system, in: Guide to Best Practices for Ocean CO2 Measurements, PICES Special Publication 3, North Pacific Marine Science Organization, Sidney, BC, Canada, 1–6, 2007a.

Dickson, A. G., Sabine, C. L., and Christian, J. R. (Eds.): SOP 6b: Determination of the pH of sea water using the indicator dye m-cresol purple, in: Guide to Best Practices for Ocean CO2 Measurements, PICES Special Publication 3, North Pacific Marine Science Organization, Sidney, BC, Canada, 1–7, 2007b.

Paulsen, M.-L. and Dickson, A. G.: Preparation of 2-amino-2-hydroxymethyl-1,3-propanediol (TRIS) pHT buffers in synthetic seawater, Limnol. Oceanogr. Methods, 18, 504–515, https://doi.org/10.1002/lom3.10383, 2020.

Rijkenberg, M. J. A., de Baar, H. J. W., Bakker, K., Gerringa, L. J. A., Keijzer, E., Laan, M., Laan, P., Middag, R., Ober, S., van Ooijen, J., Ossebaar, S., van Weerlee, E. M., and Smit, M. G.: "PRISTINE", a new high volume sampler for ultraclean sampling of trace metals and isotopes, Mar. Chem., 177, 501–509, https://doi.org/10.1016/j.marchem.2015.07.001, 2015.

4. Plastic degradation

4.1 Kinetics of plastic degradation

Pepien Rubbens

Every day, huge amounts of plastics enter the ocean but its further fate is still uncertain (Wayman and Niemann, 2021). Plastics at the sea surface are affected by the sun's UV rays, (partially) breaking the plastics down into smaller fragments, nanoplastic (i.e., particles >1µm), oligomers and smaller molecules. Some of these photodegradation products can be degraded further by microbes but the kinetics of this process are not well understood.

To study the mineralization of plastic photodegradation products, we used a stable isotope probing/ isotope tracing approach with different ^{13}C-labelled plastics. About 1 mg of labelled polymer was firstly irradiated in 50 ml sterile sea water in a quartz bottle with UV light with a similar wave spectrum than solar UV light but at an intensity of 25-fold higher in comparison to UV irradiance in temperate regions (Goudriaan et al., 2023; Delre et al., 2023). 1 ml of this sea water, together with the released photodegradation products (in the following termed tracer solution) was then added to the marine water column samples. Potential microbially mediated mineralization then quantitatively transforms the isotopically labelled polymer to CO_2

$$^{13}C_n\text{-poly} + O_2 \rightarrow n^{13}CO_2 + R \qquad \text{(eqaution 4.1.-1)}$$

This allows calculating microbial degradation kinetics (Goudriaan et al., 2023) and thus to assess the potential turnover time of the plastic photodegradation products.

Table 4.1-1: Number of vials (#V) terminated (term) at every timestep (t_1-t_5) per temperature and per depth.

Polymer	#V total	#V t_1	#V t_2	#V t_3	#V t_4	#V t_5
PP	15	3	3	3	3	3
PE	15	3	3	3	3	3
PS	15	3	3	3	3	3
PET	15	3	3	3	3	3
Control	15	3	3	3	3	3

For the experiment performed during PE-525, we incubated water column samples at ambient (14,5°C) and room temperature on board with a tracer solution inoculum of Polyethylene (PE), Polypropylene (PP), Polystyrene (PS) and Polyester (PET), see table 1. The negative control contained solely seawater. Incubations were terminated at successive time steps to monitor the accumulation of $^{13}CO_2$ in the headspace for assessing kinetics in accordance to equation 4.1.-1.

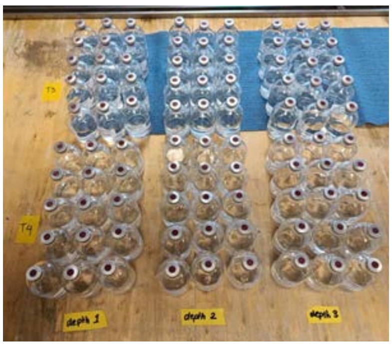

Figure 4.1.-2: Incubation vials from t_3 and t_4 for one incubation temperature.

Sample collection and experimental procedure

Seawater samples were collected using a CTD with 24 Niskin bottles at the location A15-3. Incubations were carried out with seawater from 30m, 15m and the sea surface (5m), directly tapped from Niskin bottles. For a given combination of depth, time and polymer type, 70 ml aliquots were filled into 100 ml serum vials, in triplicate. After the tracer solution was added, the vials were sealed with a halogenated butyl rubber (for each time step, 15 individual incubations were thus prepared per polymer). After 1, 6, 11, 16 and 21 days of incubation, T1-T5 respectively, sets were terminated by adding 0.1ml of $HgCl_2$

to stop further microbial activity and to preserve conditions for measuring headspace CO_2 concertation and stable isotope composition at NIOZ. Figure 4.1.-1 shows a subset of the vials that were used during this experiment.

Bibliography

Delre, A.; Goudriaan, M.; Hernando Morales, V.; Vaksmaa, A.; Ndhlovu Tintswalo, R.; Baas, M.; Keijzer, E.; de Groot, T.; Zeghal, E.; Egger, M.; Röckmann, T.; Niemann, H. Plastic photodegra-dation under simulated marine conditions. Marine Pollution Bulletin, doi.org/10.1016/j.marpolbul.2022.114544 (2023).

Goudriaan, M.; Hernando Morales, V.; van der Meer, M. T. J.; Mets, A.; Ndhlovu Tintswalo, R.; van Heerwaarden, J.; Simon, S.; Heuer, V. B.; Hinrichs, K.-U.; Niemann, H. *A stable isotope assay with 13C-labeled polyethylene to investigate plastic mineralization mediated by Rhodococcus ruber.* Marine Pollution Bulletin, doi.org/10.1016/j.marpolbul.2022.114369 (2023).

Wayman, C. & Niemann, H. The fate of plastic in the ocean environment – a minireview, Environmental Science: Processes & Impacts, doi.org/10.1039/D0EM00446D

5. Nutrients

Annalisa Delre, Yasmina Ourradi, Jessica Riekenberg

The nutrient samples were firstly collected through a long silicone tube in 60 ml syringes rinsed three times before being filled and numbered 1 to 24 and corresponding to the PRISTINE bottles. Once in the laboratory, the content of the syringes was filtered into a 6 ml polyethylene vials that were rinsed 3 times before filling. The samples for ammonium, phosphate, nitrate and nitrite analysis were frozen at approximately -20°C and the silicate samples were stored in the fridge at 4-8°C in the dark. The nutrient samples will be analysed at NIOZ.

Appendix

The appendix comprises a detailed list of all echosounder surveys and a complete station list

Multibeam (EM302 or EM2040) and water column echo sounder (EK80) flare surveys

Night 17/18 October 2023 **<u>EK80 frequency: 200 kHz only</u>**

Time	Echo sounder		Start	Stop	Remarks
(UTC)	EK80	EM2040			
19:18		x	x		Line 3, no bubbles
19:24		x		x	
19:42		x	x		Line 4, bubbles
19:48		x		x	
20:06	x		x		bubbles
20:12	x			x	
20:47		x	x		Line 6, weak bubbles,
20:51		x		x	water columnn logging started little bit later
21:08	x		x		no bubbles (probabaly just off line)
21:11	x			x	
21:47		x	x		Line 8, few bubbles
21:50		x		x	
22:08	x		x		bubbles
22:11	x			x	
22:44		x	x		Line 9, few bubbles
22:47		x		x	
23:07	x		x		bubbels
23:11	x			x	
23:45		x	x		Line 10, few bubbles
23:49		x		x	
00:06	x		x		no bubbles (probabaly just off line)
00:13	x			x	
00:44		x	x		Line 11. few bubbels
00:48		x		x	
01:07	x		x		large plume
01:12	x			x	
01:43		x	x		Line 12, few bubbles
01:48		x		x	
02:06	x		x		large plume
02:10	x			x	

Multibeam (EM302 or EM2040) and water column echo sounder (EK80) flare surveys

Night 23/24 October 2023 **EK80 frequency: 70 & 200 kHz**

Time	Echo sounder		Start	Stop	Remarks
(UTC)	EK80	EM302			
18:45		x	x		E-->W
18:49		x		x	Line 45
19:07	x		x		E-->W
19:10	x			x	no plume
19:28	x		x		W-->E
19:33	x			x	large plume
19:50		x	x		W-->E
19:54		x		x	Line 46
20:10	x		x		W-->E
20:14	x			x	large plume
20:22	x		x		E-->W
20:25	x			x	small plume
20:45		x	x		W-->E
20:49		x		x	Line 47
21:04	x		x		W-->E
21:08	x			x	large plume
21:46		x	x		W-->E
21:50		x		x	Line 48
22:05	x		x		W-->E
22:09	x			x	plume
22:45		x	x		W-->E
22:49		x		x	Line 49
23:03	x		x		W-->E
23:07	x			x	plume
23:45		x	x		W-->E
23:49		x		x	Line 50
00:05	x		x		W-->E
00:09	x			x	3 plumes
00:44		x	x		W-->E
00:49		x		x	Line 51
01:05	x		x		W-->E
01:09	x			x	3 plumes
01:44		x	x		W-->E
01:49		x		x	Line 52
02:02	x		x		W-->E
02:10	x			x	plume

Multibeam (EM302 or EM2040) and water column echo sounder (EK80) flare surveys

Night 24-25 October 2023 **EK80 frequency: 70 & 200 kHz**

Time	Echo sounder		Start	Stop	Remarks
(UTC)	EK80	EM302			
18:35		x	x		E-->W, line 55
18:43		x		x	no bubbles A18-EBU4 locatation 1
18:55		x	x		W-->E, line 56
19:02		x		x	no bubbles
18:55	x		x		W-->E, same time as EM302
18:59	x			x	stopped halfway, no bubbles
19:11		x	x		E-->W, line 57
19:18		x		x	no bubbles
19:26		x	x		W-->E, line 58
19:33		x		x	no bubbles
Move to new location					
19:53		x	x		E-->W, line 59
19:56		x		x	no bubbles
20:05		x	x		W-->E, line 60
20:08		x		x	no bubbles
20:17		x	x		W-->W, line 61
20:19		x		x	no bubbles

Multibeam (EM302 or EM2040) and water column echo sounder (EK80) flare surveys

Seapath regularly shows reduced positioin and rol/pitch
General Seapth data quality is `green`

Night 26/27 October 2023 **EK80 frequency: 70 & 200 kHz**

Sheet 1

Time	Echo sounder		Start	Stop	Remarks
(UTC)	EM2040	EK80			
17:58	x		x		plume, line 13
18:04	x			x	NW-->SE, strong wind
18:29		x	x		NW-->SE, stron wind
18:33		x		x	no plume
18:50	x		x		NW-->SE, line 14
18:55	x			x	strong wind, plume
19:14		x	x		NW-->SE
19:18		x		x	strong wind, partial plume
19:50	x		x		NW-SE, line 15
19:54	x			x	plume
20:13		x	x		NW-->SE
20:17		x		x	strong wind, partial plume
20:51	x		x		NW-->SE, line 16
20:55	x			x	good tracvk: complete plume
21:13		x	x		NW-->SE
21:18		x		x	comple plume: 55°01.817'N 004°31.393'E
21:54	x		x		NW-->SE, line 17
21:56	x			x	plume
22:14		x	x		NW-->SE
22:20		x		x	small plume
22:50	x		x		NW-->SE, line 18
22:56	x			x	plume
23:18		x	x		NW-->SE
23:23		x		x	no plume
23:49	x		x		NW-->SE, line 19
23:55	x			x	vague plume(?), too long track (return track)
00:16		x	x		pinging started late
00:22		x		x	NW-->SE, no pume
00:50	x		x		WNW-->ESE, line 20, no plume
00:57	x			x	coarse change because of wind
01:18		x	x		WNW-->ESE, no plume, engine overheat warning
01:26		x		x	-->pull back engine, ship moves backwards (01:23)
01:49	x		x		WNW-->ESE, line 21
01:54	x			x	no plume
02:14		x	x		strong wind (7Bft) --> difficulties manouvring
02:19		x		x	no plume

Multibeam (EM302 or EM2040) and water column echo sounder (EK80) flare surveys

Night 26/27 October 2023 **EK80 frequency: 70 & 200 kHz**

Sheet 2

Time	Echo sounder		Start	Stop	Remarks
(UTC)	EM2040	EK80			
02:38	x		x		plume(?), line 22
02:43	x			x	WNW-->ESE
03:02		x	x		WNW-->ESE
03:06		x		x	no plume
03:44	x		x		WNW-->ESE, line 23
03:47	x			x	no plume
04:05		x	x		WNW-->ESE
04:09		x		x	no plume
04:41	x		x		WNW-->ESE line 24
04:45	x			x	weak plume?
05:04		x	x		WNW-->ESE
05:08		x		x	most probably 2 plumes (not at seabed)

Multibeam (EM302 or EM2040) and water column echo sounder (EK80) flare surveys

B17-04, natural seepage, second time

Night 27/28 October 2023 **EK80 frequency: 70 & 200 kHz**

Sheet 1

Time	Echo sounder		Start	Stop	Remarks
(UTC)	EM2040	EK80			Regularly air underneath the transducers
18:28	x		x		WNW-->ESE, line 26
18:32	x			x	plumes
18:48		x	x		WNW-->ESE
18:52		x		x	plumes
19:28	x		x		WNW-->ESE, line 27
19:32	x			x	plumes
19:48		x	x		WNW-->ESE
19:52		x		x	3 plumes
20:29	x		x		WNW-->ESE, line 28
20:33	x			x	plumes
20:49		x	x		WNW-->ESE
20:53		x		x	plumes
21:30	x		x		WNW-->ESE, line 29
21:35	x			x	polumes
21:51		x	x		WNW-->ESE
21:57		x		x	large plume
22:29	x		x		WNW-->ESE, line 31
22:35	x			x	plumes
22:55		x	x		WNW-->ESE
23:02		x		x	large plume
23:30	x		x		WNW-->ESE, line 32
23:36	x			x	small plume
23:53		x	x		WNW-->ESE
23:59		x		x	(margin of) plumes
00:30	x		x		WNW-->ESE, lined 33
00:35	x			x	weak plumes
00:51		x	x		WNW-->ESE. (margin of) plumes, EK80 sometimes
00:57		x		x	stops pinging (work overload processor?)
Change course					
01:30	x		x		NE-->SE,m line 34
01:37	x			x	weak plumes
01:55		x	x		NW-->SE
02:02		x		x	geen pluimen

Multibeam (EM302 or EM2040) and water column echo sounder (EK80) flare surveys

B17-04, natural seepage, second time

Night 27/28 October 2023 **EK80 frequency: 70 & 200 kHz**

Sheet 2

Time	Echo sounder		Start	Stop	Remarks
(UTC)	EM2040	EK80			Regularly air underneath the transducers
02:32	x		x		NW-->SE, line 35
02:38	x			x	weak plumes?, strong wind-->off course
02:54		x	x		NW-->SE
02:58		x		x	no plumes
03:29	x		x		NW-->SE, line 36
03:34	x			x	clear plumes
03:52		x	x		NW-->SE
03:55		x		x	plumes
04:26	x		x		NW-->SE, line 37
04:30	x			x	plumes
04:46		x	x		NW-->SE
04:51		x		x	plumes

Multibeam (EM302 or EM2040) and water column echo sounder (EK80) flare surveys

A15-03, second time

Night 28/29 October 2023 **EK80 frequency: 70 & 200 kHz**

Sheet 1

Time	Echo sounder		Start	Stop	Remarks
(UTC)	EM2040	EK80			
18:42	x		x		N-->S, line 38
18:47	x			x	pl,ume
19:04		x	x		NE-->SW
19:10		x		x	plume touching seabed
19:46	x		x		NE-->SW, line 39
19:51	x			x	plume
20:06		x	x		NE-->SW
20:11		x		x	plume
20:44	x		x		NE-->SW, line 40
20:48	x			x	partial plume
21:04		x	x		NE-->SW
21:09		x		x	partial plume
21:45	x		x		N-->S, line 41
21:48	x			x	plume
22:04		x	x		N-->S
22:09		x		x	large plume
22:45	x		x		NW-->SE, line 42
22:49	x			x	plume
23:08		x	x		NW-->SE
23:11		x		x	large plume
23:44	x		x		NNW-->SSE, line 43
23:48	x			x	large plume
00:09		x	x		NNW-->SSE
00:13		x		x	large plume
00:45	x		x		NNW-->SSE, line 44
00:49	x			x	plume
01:09		x	x		NNW-->SSE
01:13		x		x	partial plume
01:44	x		x		NNW-->SSE, line 45
01:48	x			x	large plume (maybe 2?)
02:08		x	x		NNW--<SSE, wind increases and changes direction
02:12		x		x	partial plume (02:10:36)
02:44	x		x		NW-->SE, line 46
02:49	x			x	plume (2?), current appears towards SW
03:07		x	x		NW-->SE
03:11		x		x	plume (part just above seabed, 03:09:12)

Multibeam (EM302 or EM2040) and water column echo sounder (EK80) flare surveys

A15-03, second time

Night 28/29 October 2023 **EK80 frequency: 70 & 200 kHz**

Sheet 2

Time	Echo sounder		Start	Stop	Remarks
(UTC)	EM2040	EK80			
03:45	x		x		NW-->SE, line 47
03:49	x			x	plume unclear
04:08		x	x		NW-->SE
04:12		x		x	pluim
04:44	x		x		WNW-->ESE, line 48, 7Bft, strongly variable wind
04:48	x			x	plume
05:07		x	x		WNE-->ESE
05:11		x		x	plume
05:42	x		x		WNW-->ESE, line 49, 7Bft
05:46	x			x	plume, bumpy waves, foam undefr transducers
06:03		x	x		WNW-->ESE, bumpy waves
06:07		x		x	plume near seabed, fgioam under stransducers

Multibeam (EM302 or EM2040) and water column echo sounder (EK80) flare surveys

A8-01, two locations

Daytime 29 October 2023 **EK80 frequency: 70 & 200 kHz**

Time	Echo sounder		Start	Stop	Remarks
(UTC)	EM2040	EK80			Roll/pitch & heave always reduced, artefacts
10:14	x		x		NW-->SE, line 50
10:19	x			x	small plumes?
10:34		x	x		NW-->SE
10:41		x		x	no plume
10:59	x		x		NW-->SE, line 51
11:04	x			x	plume
11:20		x	x		NW-->SE
11:26		x		x	plume site just missed
New location					
12:02	x		x		N--->S, linme 52
12:06	x			x	no plumes
12:25	x		x		N-->S line 53
12:29	x			x	no plumes

Appendix (PE-525)

Date	*latitude*	*longitude*	*Phase name*	*Device name*	*Action name*	*Operation Id*	*Cast*	*Location*	*comment*
16/10/2023 08:25	**55.3002**	**3.8273**	STATION 1	Multibeam	BEGIN	64PE525EM3021	1_1	A15-3	
16/10/2023 13:20	**55.3038**	**3.8178**	STATION 1	Multibeam	END	64PE525EM3021	1_2		
16/10/2023 14:26	**55.3008**	**3.8265**	STATION 2	Flooting Chamber	START	64PE525FLCHM2	2_1		
16/10/2023 15:19	**55.3007**	**3.8265**	STATION 2	Flooting Chamber	STOP	64PE525FLCHM2	2_3		
17/10/2023 06:12	**55.3003**	**3.8265**	STATION 3	CTD	BOT	64PE525CTD3	3_1		
17/10/2023 08:15	**55.3005**	**3.8268**	STATION 4	CTD	BOT	64PE525CTD4	4_1		
17/10/2023 09:02	**55.3005**	**3.8263**	STATION 5	Flooting Chamber	BEGIN	64PE525FLCHM5	5_1		
17/10/2023 09:30	**55.3003**	**3.8258**	STATION 5	Flooting Chamber	STOP	64PE525FLCHM5	5_1		
17/10/2023 09:51	**55.3005**	**3.8265**	STATION 6	CTD	BOT	64PE525CTD6	6_1		
17/10/2023 11:10	**55.3003**	**3.826**	STATION 7	Flooting Chamber	START	64PE525FLCHM7	7_1		
17/10/2023 11:41	**55.3002**	**3.826**	STATION 7	Flooting Chamber	STOP	64PE525FLCHM7	7_1		
17/10/2023 11:58	**55.3005**	**3.8263**	STATION 8	CTD	BOT	64PE525CTD8	8_1		
17/10/2023 12:42	**55.3003**	**3.826**	STATION 9	ROV deployment	DEP	64PE525ROVDEP9	9_1		
17/10/2023 14:06	**55.3005**	**3.8263**	STATION 10	CTD	BOT	64PE525CTD10	10_1		
17/10/2023 14:49	**55.3007**	**3.8263**	STATION 11	ROV deployment	DEP	64PE525ROVDEP11	11_1		
17/10/2023 15:55	**55.3005**	**3.8265**	STATION 12	CTD	BOT	64PE525CTD12	12_1		

17/10/2023 16:43	**55.3003**	**3.8265**	STATION 13	ROV deployment	DEP	64PE525ROVDEP13	13_1		
17/10/2023 18:01	**55.3005**	**3.8268**	STATION 14	CTD	BOT	64PE525CTD14	14_1		
17/10/2023 19:19	**55.2995**	**3.825**	STATION 15	Multibeam	BEGIN	64PE525EM30215	15_1		
18/10/2023 02:20	**55.3017**	**3.8238**	STATION 15	Multibeam	END	64PE525EM30215	15_1		
18/10/2023 06:04	**55.3005**	**3.8263**	STATION 16	CTD	BOT	64PE525CTD16	16_1		
18/10/2023 07:03	**55.3005**	**3.8263**	STATION 17	ROV deployment	DEP	64PE525ROVDEP17	17_1		
18/10/2023 10:12	**55.3005**	**3.8263**	STATION 18	ROV deployment	END	64PE525ROVDEP17	17_1		
18/10/2023 09:00	**55.3005**	**3.8265**	STATION 18	SLURF	BEGIN	64PE525SLURFER18	18_1		
18/10/2023 10:03	**55.3007**	**3.8263**	STATION 18	SLURF	END	64PE525SLURFER18	18_19		
18/10/2023 11:26	**55.3005**	**3.8265**	STATION 19	CTD	BOT	64PE525CTD19	19_1		
22/10/2023 10:00	**55.3003**	**3.8263**	STATION 20	Lander BOBO	DEP	64PE525LANDBOBO20	20_2		
22/10/2023 17:07	**55.3005**	**3.8262**	STATION 22	ROV deployment	DEP	64PE525ROVDEP22	22_1		
23/10/2023 06:04	**55.0332**	**4.4813**	STATION 24	CTD	BOT	64PE525CTD24	24_1	B17-4	
23/10/2023 07:55	**55.0333**	**4.4813**	STATION 25	ROV deployment	REC	64PE525ROVDEP25	25_1		
23/10/2023 08:09	**55.0333**	**4.4815**	STATION 26	CTD	BOT	64PE525CTD26	26_1		on place, flare
23/10/2023 08:55	**55.0332**	**4.481**	STATION 27	Flooting Chamber	BEGIN	64PE525FLCHM27	27_1		
23/10/2023 09:29	**55.0332**	**4.4812**	STATION 27	Flooting Chamber	END	64PE525FLCHM27	27_1		
23/10/2023 09:45	**55.0333**	**4.4812**	STATION 28	CTD	BOT	64PE525CTD28	28_1		on palce

23/10/2023 12:48	**55.0332**	**4.4813**	STATION 29	ROV deployment	DEP	64PE525ROVDEP29	29_1	
23/10/2023 13:06	**55.0333**	**4.4815**	STATION 29	SLURF	START	64PE525SLURFER29	29_2	
23/10/2023 13:32	**55.0333**	**4.4815**	STATION 29	SLURF	STOP	64PE525SLURFER29	29_2	
23/10/2023 14:14	**55.0332**	**4.4813**	STATION 30	CTD	BOT	64PE525CTD30	30_1	on place
23/10/2023 14:30	**55.0332**	**4.4813**	STATION 31	Flooting Chamber	START	64PE525FLCHM31	31_1	
23/10/2023 14:36	**55.0332**	**4.4812**	STATION 31	Flooting Chamber	STOP	64PE525FLCHM31	31_1	
23/10/2023 14:40	**55.0332**	**4.4813**	STATION 31	Flooting Chamber	START	64PE525FLCHM31	31_2	
23/10/2023 14:54	**55.0332**	**4.4815**	STATION 31	Flooting Chamber	STOP	64PE525FLCHM31	31_2	
23/10/2023 14:58	**55.0332**	**4.4813**	STATION 31	Flooting Chamber	START	64PE525FLCHM31	31_3	
23/10/2023 15:10	**55.033**	**4.4812**	STATION 31	Flooting Chamber	STOP	64PE525FLCHM31	31_3	
23/10/2023 15:16	**55.0332**	**4.4815**	STATION 31	Flooting Chamber	START	64PE525FLCHM31	31_4	
23/10/2023 15:24	**55.0333**	**4.4818**	STATION 31	Flooting Chamber	STOP	64PE525FLCHM31	31_4	
23/10/2023 15:56	**55.0333**	**4.4818**	STATION 32	CTD	BOT	64PE525CTD32	32_1	on place
23/10/2023 16:43	**55.0335**	**4.4817**	STATION 33	ROV deployment	DEP	64PE525ROVDEP33	33_1	
23/10/2023 17:34	**55.0337**	**4.4815**	STATION 34	CTD	BOT	64PE525CTD34	34_1	on place
23/10/2023 18:44	**55.0335**	**4.4847**	STATION 35	Multibeam	BEGIN	64PE525EM30235	35_1	
23/10/2023 18:57	**55.0345**	**4.4803**	STATION 35	Multibeam	END	64PE525EM30235	35_1	
23/10/2023 19:10	**55.0332**	**4.4798**	STATION 35	Multibeam	BEGIN	64PE525VMADCP35	35_2	
23/10/2023 19:10	**55.0333**	**4.4798**	STATION 35	Multibeam	END	64PE525VMADCP35	35_2	
23/10/2023 19:28	**55.0333**	**4.4802**	STATION 35	Multibeam	BEGIN	64PE525VMADCP35	35_3	
23/10/2023 19:33	**55.0333**	**4.4847**	STATION 35	Multibeam	END	64PE525VMADCP35	35_3	

23/10/2023 19:49	**55.0333**	**4.4793**	STATION 35	Multibeam	BEGIN	64PE525EM30235	35_4	
24/10/2023 02:10	**55.0333**	**4.4847**	STATION 35	Multibeam	END	64PE525EM30235	35_4	
24/10/2023 02:50	**55.0303**	**4.5207**	STATION 36	Multibeam	BEGIN	64PE525EM30236	36_1	
24/10/2023 03:35	**55.0228**	**4.5168**	STATION 36	Multibeam	END	64PE525EM30236	36_1	
24/10/2023 06:04	**55.0347**	**4.4808**	STATION 37	CTD	BOT	64PE525CTD37	37_1	wrong, is on nav point not on flare
24/10/2023 06:05	**55.0345**	**4.4805**	STATION 38	Flooting Chamber	BEGIN	64PE525FLCHM38	38_1	stop, weather too choppy
24/10/2023 06:12	**55.0343**	**4.4803**	STATION 38	Flooting Chamber	STOP	64PE525FLCHM38	38_1	
24/10/2023 07:55	**55.035**	**4.4805**	STATION 39	CTD	BOT	64PE525CTD39	39_1	wrong, is on nav point
24/10/2023 08:52	**55.035**	**4.4805**	STATION 40	SLURF	START	64PE525SLURFER40	40_1	
24/10/2023 10:06	**55.0348**	**4.48**	STATION 40	SLURF	STOP	64PE525SLURFER40	40_1	
24/10/2023 11:11	**55.0348**	**4.4805**	STATION 41	CTD	BOT	64PE525CTD41	41_1	wrong, is on nav point
24/10/2023 12:08	**55.0348**	**4.4805**	STATION 42	SLURF	START	64PE525SLURFER42	42_	
24/10/2023 12:52	**55.0348**	**4.481**	STATION 42	SLURF	STOP	64PE525SLURFER42	42_1	
24/10/2023 13:02	**55.035**	**4.4808**	STATION 43	CTD	BOT	64PE525CTD43	43_1	wrong, is on nav point
24/10/2023 13:58	**55.0343**	**4.4807**	STATION 44	ROV deployment	DEP	64PE525ROVDEP44	44_1	
24/10/2023 18:35	**55.1165**	**3.7725**	STATION 45	Multibeam	BEGIN	64PE525EM30245	45_1	
24/10/2023 19:37	**55.1185**	**3.7737**	STATION 45	Multibeam	END	64PE525EM30245	45_1	
24/10/2023 19:51	**55.1253**	**3.7637**	STATION 46	Multibeam	BEGIN	64PE525EM30246	46_1	
24/10/2023 20:21	**55.1245**	**3.757**	STATION 46	Multibeam	END	64PE525EM30246	46_1	
25/10/2023 08:16	**55.3005**	**3.8262**	STATION 47	Lander BOBO	END	64PE525LANDBOBO47	47_1	Lander recovery A15-3

25/10/2023 06:51	**55.3003**	**3.8262**	STATION 47	ROV deployment	BEGIN	64PE525ROVDEP47	47_2		
25/10/2023 14:17	**55.0332**	**4.4822**	STATION 48	Lander BOBO	DEP	64PE525LANDBOBO48	48_1		B17-4 lander pos: 55.03319633; 4.48217200
26/10/2023 06:05	**55.0303**	**4.5232**	STATION 49	CTD	BOT	64PE525CTD49	49_1	B17-5	
26/10/2023 06:21	**55.0305**	**4.5233**	STATION 50	Flooting Chamber	START	64PE525FLCHM50	50_1		
26/10/2023 08:30	**55.0302**	**4.5232**	STATION 51	Flooting Chamber	END	64PE525FLCHM50	50_1		
26/10/2023 08:06	**55.0302**	**4.5225**	STATION 51	CTD with Samples	BOT	64PE525CTDBOT51	51_1		
26/10/2023 08:55	**55.0305**	**4.523**	STATION 52	SLURF	START	64PE525SLURFER52	52_1		
26/10/2023 09:20	**55.0302**	**4.5232**	STATION 52	SLURF	STOP	64PE525SLURFER52	52_1		
26/10/2023 09:33	**55.0303**	**4.5237**	STATION 53	CTD with Samples	BOT	64PE525CTDBOT53	53_1		
26/10/2023 11:06	**55.0303**	**4.5233**	STATION 54	SLURF	BEGIN	64PE525SLURFER54	54_1		
26/10/2023 11:27	**55.0303**	**4.5233**	STATION 54	SLURF	END	64PE525SLURFER54	54_1		
26/10/2023 11:33	**55.0303**	**4.5233**	STATION 55	CTD	BOT	64PE525CTD55	55_1		
26/10/2023 12:28	**55.0303**	**4.5235**	STATION 56	ROV deployment	DEP	64PE525ROVDEP56	56_1		
26/10/2023 13:57	**55.0303**	**4.5233**	STATION 57	CTD	BOT	64PE525CTD57	57_1		
26/10/2023 16:32	**55.0302**	**4.5235**	STATION 58	ROV deployment	REC	64PE525ROVDEP58	58_1		
26/10/2023 16:39	**55.0302**	**4.5233**	STATION 59	CTD	BOT	64PE525CTD59	59_1		
26/10/2023 17:58	**55.0313**	**4.52**	STATION 60	Multibeam	BEGIN	64PE525EM30260	60_		

27/10/2023 05:09	**55.0297**	**4.5277**	STATION 60	Multibeam	END	64PE525EM30260	60_1	
27/10/2023 06:03	**55.0305**	**4.5232**	STATION 61	CTD	BOT	64PE525CTD61	61_1	
27/10/2023 07:00	**55.0305**	**4.5232**	STATION 62	SLURF	START	64PE525SLURFER62	62_1	
27/10/2023 07:36	**55.0305**	**4.5232**	STATION 62	SLURF	STOP	64PE525SLURFER62	62_1	
27/10/2023 07:47	**55.0305**	**4.5228**	STATION 63	CTD with Samples	BOT	64PE525CTDBOT63	63_1	
27/10/2023 08:39	**55.0308**	**4.523**	STATION 64	SLURF	START	64PE525SLURFER64	64_1	
27/10/2023 09:24	**55.0307**	**4.5233**	STATION 64	SLURF	STOP	64PE525SLURFER64	64_1	
27/10/2023 09:34	**55.0308**	**4.5232**	STATION 65	CTD with Samples	BOT	64PE525CTDBOT65	65_1	
27/10/2023 11:45	**55.0303**	**4.5233**	STATION 66	CTD with Samples	BOT	64PE525CTDBOT66	66_1	
27/10/2023 12:39	**55.0303**	**4.5233**	STATION 67	SLURF	START	64PE525SLURFER67	67_1	
27/10/2023 13:22	**55.0305**	**4.5233**	STATION 67	SLURF	STOP	64PE525SLURFER67	67_1	
27/10/2023 13:31	**55.0305**	**4.5223**	STATION 68	CTD with Samples	BOT	64PE525CTDBOT68	68_1	
27/10/2023 15:30	**55.0335**	**4.482**	STATION 69	Lander BOBO	REC	64PE525LANDBOBO69	69_1	B17-4
27/10/2023 18:28	**55.0337**	**4.4797**	STATION 70	Multibeam	BEGIN	64PE525EM30270	70_1	
28/10/2023 04:59	**55.0328**	**4.4805**	STATION 70	Multibeam	END	64PE525EM30270	70_1	
28/10/2023 06:04	**55.0333**	**4.4815**	STATION 71	CTD	BOT	64PE525CTD71	71_1	
28/10/2023 06:58	**55.0335**	**4.4822**	STATION 72	SLURF	START	64PE525SLURFER72	72_1	

28/10/2023 07:41	**55.033**	**4.4812**	STATION 72	SLURF	END	64PE525SLURFER72	72_1		
28/10/2023 07:46	**55.0333**	**4.4815**	STATION 73	CTD with Samples	BOT	64PE525CTDBOT73	73_1		
28/10/2023 08:33	**55.0335**	**4.482**	STATION 74	SLURF	BEGIN	64PE525SLURFER74	74_1		
28/10/2023 09:24	**55.0335**	**4.4818**	STATION 74	SLURF	END	64PE525SLURFER74	74_1		
28/10/2023 09:31	**55.0333**	**4.4818**	STATION 75	CTD with Samples	BOT	64PE525CTDBOT75	75_1		
28/10/2023 11:34	**55.0335**	**4.4817**	STATION 76	CTD with Samples	BOT	64PE525CTDBOT76	76_1		
28/10/2023 14:13	**55.0302**	**4.5233**	STATION 77	Lander BOBO	DEP	64PE525LANDBOBO77	77_1	B17-5	
28/10/2023 18:14	**55.3022**	**3.8235**	STATION 78	Multibeam	BEGIN	64PE525EM30278	78_1	A15-03	
29/10/2023 06:08	**55.2998**	**3.8318**	STATION 78	Multibeam	END	64PE525EM30278	78_1		
29/10/2023 07:12	**55.3005**	**3.8265**	STATION 79	Boxcore d=300	BOT	64PE525BOX30079	79_1		sandy, silty, some reduced veins but no sulphidic smell
29/10/2023 10:09	**55.5367**	**3.6287**	STATION 80	Multibeam	BEGIN	64PE525EM30280	80_1	A08-01	
29/10/2023 12:36	**55.5388**	**3.6348**	STATION 80	Multibeam	END	64PE525EM30280	80_1		
30/10/2023 09:05	**55.1668**	**4.3337**	STATION 81	Boxcore d=300	BOT	64PE525BOX30081	81_1	Ref stat	sandy, silty, some reduced veins but no sulphidic smell
30/10/2023 09:35	**55.167**	**4.3342**	STATION 82	CTD with Samples	BOT	64PE525CTDBOT82	82_1		
30/10/2023 10:31	**55.1665**	**4.3333**	STATION 83	SLURF	START	64PE525SLURFER83	83_1		
30/10/2023 12:03	**55.1668**	**4.3328**	STATION 83	SLURF	STOP	64PE525SLURFER83	83_1		
30/10/2023 13:58	**55.0302**	**4.5233**	STATION 84	Lander BOBO	END	64PE525LANDBOBO84	84_1	B17-5	
30/10/2023 14:23	**55.0302**	**4.5233**	STATION 85	Boxcore d=300	BOT	64PE525BOX30085	85_1		

30/10/2023 14:54	**55.0333**	**4.4815**	STATION 86	Boxcore d=300	BOT	64PE525BOX30086	86_1	B17-4
30/10/2023 17:57	**54.7548**	**4.363**	STATION 87	Multibeam	BEGIN	64PE525EM30287	87_1	F05-06_MB_Calib
30/10/2023 19:19	**54.7568**	**4.3542**	STATION 87	Multibeam	END	64PE525EM30287	87_1	